The O_2-independent pathway of ubiquinone biosynthesis is essential for denitrification in *Pseudomonas aeruginosa*

Chau-Duy-Tam Vo[1¶], Julie Michaud[2¶], Sylvie Elsen[3], Bruno Faivre[1], Emmanuelle Bouveret[4,5], Frédéric Barras[4,5], Marc Fontecave[1], Fabien Pierrel[2], Murielle Lombard[1]* and Ludovic Pelosi[2]*

[1]Laboratoire de Chimie des Processus Biologiques, Collège de France, CNRS UMR 8229, PSL Research University, Sorbonne Université, Paris, France ; [2]CNRS, CHU Grenoble Alpes, Grenoble INP, TIMC-IMAG, Université Grenoble Alpes, Grenoble, France; [3]Biology of Cancer and Infection, U1036 INSERM, CEA, Université Grenoble Alpes, ERL5261 CNRS, Grenoble, France; [4]SAMe Unit, Department of Microbiology, Institut Pasteur, Paris, France; [5]IMM-UMR 2001 CNRS-Institut Pasteur, Paris, France

Running title: Ubiquinone is essential for denitrification in *Pseudomonas aeruginosa*

*To whom correspondence should be addressed: ludovic.pelosi@univ-grenoble-alpes.fr, murielle.lombard@college-de-france.fr

¶ C.-D.-T.V. and J.M. contributed equally to the work.

Keywords: ubiquinone biosynthesis, coenzyme Q, anaerobic respiration chain, denitrification, Pseudomonas aeruginosa, iron-sulfur protein

ABSTRACT

Many proteobacteria, such as *Escherichia coli*, contain two main types of quinones, benzoquinones represented by ubiquinone (UQ) and naphthoquinones such as menaquinone (MK) and dimethyl-menaquinone (DMK). MK and DMK function predominantly in anaerobic respiratory chains, whereas UQ is the major electron carrier used for reduction of dioxygen. However, this division of labor is probably not so stric. Indeed, a pathway that produces UQ under anaerobic conditions in an UbiU-, UbiV- and UbiT-dependent manner has been recently discovered in *E. coli*. Nevertheless, the physiological relevance of this pathway is not yet understood because of the presence of MK and DMK in this bacterium. In the present study, we established that UQ_9 is the single quinone of *P. aeruginosa* and is required for growth under anaerobic respiration (denitrification). Moreover, we demonstrated that ORFs *PA3911*, *PA3912* and *PA3913*, which are homologues to the *ubiT*, *ubiV* and *ubiU E. coli* genes in the anaerobic pathway, respectively, were essential for UQ_9 biosynthesis and thus for denitrification in *P. aeruginosa*. We showed that UbiV from *P. aeruginosa* accommodates a [4Fe-4S] cluster, as is the case with its *E. coli* homolog. Moreover, we demonstrated that UQ copurifies with UbiU. Finally, UbiT, which possesses a sterol carrier domain 2, was able to bind lipidic molecules such as UQ. Since the denitrification metabolism of *P. aeruginosa* is believed to be important for pathogenicity in cystic fibrosis patients, our results highlight the O_2-independent UQ biosynthesis pathway as a new possible target to develop innovative antibiotics.

INTRODUCTION

The opportunistic pathogen *Pseudomonas aeruginosa* has a remarkable ability to grow under a variety of environmental conditions such as soil and water as well as animal-, human-, and plant-host-associated environments. *P. aeruginosa* is responsible for numerous acute and chronic infections and presents a dramatic problem for patients with severe burns, cystic fibrosis (CF), and immunocompromising states (1,2).

The utilization of various carbon sources and energy metabolism (respiration or fermentation) might contributes to the environmental adaptation of *P. aeruginosa* (3). Its main energy-producing system is respiration, which utilizes a proton motive force (pmf) used for ATP synthesis. The pmf is produced by the transfer of electrons and protons from reduced donors to oxidized acceptors *via* the quinone pool. Whereas the dehydrogenases and reductases involved in respiratory metabolism have been well described and annotated in the genome of *P. aeruginosa* PAO1 (4,5), the composition of the quinone pool is not fully established yet in this bacterium.

Studies in the sixties suggested ubiquinone 9 (UQ_9) as a major quinone of aerobically-grown *P. aeruginosa* (6) and UQ_9 is therefore believed to be essential for aerobic respiration (7).

Proteobacteria contain two main types of quinones, benzoquinones and naphthoquinones, represented respectively by UQ (or coenzyme Q) / plastoquinone (PQ) and menaquinone (MK) / demethylmenaquinone (DMK). Typically, MK and DMK function predominantly in anaerobic respiratory chains, whereas UQ and PQ are the major electron carriers used for reduction of dioxygen by various cytochrome oxidases (8). However, the metabolic use of various quinone species according to environmental dioxygen availability might be more complex. Indeed, we recently discovered in *E. coli* a pathway that produces UQ under anaerobic conditions, and that is conserved across many bacterial species (9). The typical UQ biosynthesis pathway requires O_2 for three hydroxylation steps (10). Obviously, the flavin-dependent monooxygenases UbiI, UbiF, and UbiH, which catalyze the O_2-dependent hydroxylation steps are not involved in the anaerobic pathway, nor are the accessory UbiK and UbiJ proteins implicated in the assembly and/or stability of the aerobic Ubi complex (11). The enzymes, catalyzing the prenylation, decarboxylation and methylation of the phenyl ring of the 4-hydroxybenzoate precursor, in total seven proteins (UbiA, B, C, D, E, G, X), are common to both pathways. In addition, the anaerobic pathway requires UbiT, UbiU and UbiV proteins (9). However, as explained above, the metabolic relevance of the O_2-independent UQ pathway is not yet clearly understood to date.

In absence of O_2, *P. aeruginosa* is able to carry out anaerobic respiration with nitrate/nitrite as terminal electron acceptors of the respiratory chain. This process called denitrification allows the reduction of soluble nitrate (NO_3^-) and nitrite (NO_2^-) to gaseous nitrous oxide (N_2O) or molecular nitrogen (N_2) (12). Because *P. aeruginosa*-infected mucus in CF airway is depleted of oxygen and enriched in nitrate/nitrite, the anaerobic metabolism of *P. aeruginosa* via the denitrification pathway is believed to be important for its pathogenicity (13). Four sequential reactions involving metalloenzymes are needed to reduce nitrate to N_2, i.e. nitrate reductase, nitrite reductase, nitric oxide reductase and nitrous oxide reductase. *P. aeruginosa* was considered as a paradigm of the denitrification pathway and all the reductases involved in this metabolism have been widely studied as well as the regulatory network controlling the denitrification genes (3,4,14). However, the anaerobic quinone pool of *P. aeruginosa* has not been characterized so far.

In the present study, we discovered that UQ_9 is essential for the growth of *P. aeruginosa* PAO1 strain in denitrification medium. We identified in this bacterium the ORFs *PA3911*, *PA3912* and *PA3913* as homologs to the genes *ubiT*, *ubiV* and *ubiU*, respectively. Our results showed that these three genes hereafter called $ubiT_{Pa}$, $ubiV_{Pa}$ and $ubiU_{Pa}$ are essential components of the O_2-independent UQ_9 biosynthetic pathway of *P. aeruginosa*. We demonstrated that i), $UbiV_{Pa}$ bind a [4Fe-4S] cluster and ii) $UbiU_{Pa}$ and $UbiT_{Pa}$, copurify with UQ recognizing the isoprenoid tail. This molecular pathway for UQ production is present only in proteobacteria (9) and is for some of them essential in anaerobic conditions, as demonstrated in the present study. Taken together, our results highlight that this pathway could be an interesting lead for the development of antibiotics targeting the denitrification metabolism.

RESULTS

UQ_9 is the single quinone of *P. aeruginosa*.

The quinone content of *P. aeruginosa* PAO1, grown under ambient air or anaerobiosis (denitrification), was determined using electrochemical detection of lipid extracts separated by HPLC and compared to those obtained from *E. coli*. Whatever the conditions of growth, a single quinone species eluting at 11.5 min was present in the analyses of *P. aeruginosa* lipid extracts, UQ_{10} being used as standard (Fig. 1A and 1B). Mass spectrometry analysis showed a predominant ammonium adduct ($M+NH_4^+$) with *m/z* ratio of 812.7 (Fig. 1C), together with minor adducts such as Na^+ (817.6) and H^+ (795.7) (Fig. S1). These masses identify UQ_9 (monoisotopic mass 794.6) as the quinone produced by *P. aeruginosa*. Membranes of *E. coli* contain UQ_8 and naphthoquinones (DMK_8 and MK_8). The absence of detectable level of naphthoquinones in *P. aeruginosa* lipid extracts, with or without oxygen (Fig.1A and 1B), is in agreement with the absence of their biosynthetic pathways (MK or futalosine pathways) in *P. aeruginosa* genomes. It is also interesting to note that the UQ content of *E. coli* was superior under aerobiosis compared to anaerobiosis (97±4 *versus* 42±6 pmol of UQ_8 per mg of cells), whereas we found the opposite for *P. aeruginosa* (95±4 *versus* 126±4 pmol of UQ_9 per mg of cells). Together, our results establish

that UQ_9 is the single quinone of *P. aeruginosa* PAO1 and suggest that UQ_9 is used under denitrification conditions.

Identification of *ubi* genes in the genome of *P. aeruginosa* PAO1.

To identify the Ubi proteins of *P. aeruginosa*, IspB, UbiX, and UbiA to UbiK from *E. coli* MG1655 were first screened for homologs in the *P. aeruginosa* PAO1 protein sequence data set available at http://www.pseudomonas.com/ using the BLASTP software. As listed in Table S1 the analysis disclosed the presence of 11 homologous proteins (IspB, UbiA to UbiE, UbiG to UbiJ and UbiX). As reported previously, the functional homolog of UbiF is a Coq7-like hydroxylase (15) and the corresponding PA0655 protein was shown to be essential for aerobic UQ_9 biosynthesis (16). Overall, we propose that the O_2-dependent UQ biosynthetic pathways in *P. aeruginosa* and *E. coli* share a similar pattern (Fig. S2).

Under anaerobiosis, *E. coli* still synthesizes UQ and we recently showed that the identified three genes that we called *ubiT*, *ubiV* and *ubiU*, as essential for this process (9). Homologues of *ubiT*, *ubiV* and *ubiU* were also identified in *P. aeruginosa* PAO1 and correspond to ORFs PA3911, PA3912 and PA3913, respectively (Table S1 and Fig. S2). These genes were called hereafter $ubiT_{Pa}$, $ubiV_{Pa}$ and $ubiU_{Pa}$. Interestingly, the three genes are predicted to form an operon, *ubiUVT* (www.pseudomonas.com). They are located downstream of the genes *moeA1*, *moaB1*, *moaE*, *moaD* and *moaC* involved in the biosynthesis of the molybdopterin cofactor (MoCo) (Fig. S3). MoCo is essential for nitrate reductase activity (17). Next, we evaluated the metabolic relevance of the O_2-independent UQ biosynthetic pathway in *P. aeruginosa* by studying mutants of $ubiT_{Pa}$, $ubiU_{Pa}$ and $ubiV_{Pa}$ genes.

Tn mutants of $ubiV_{Pa}$ and $ubiU_{Pa}$ present a growth defect for denitrification and impaired UQ_9 content.

The physiological importance of the proteins $UbiT_{Pa}$, $UbiU_{Pa}$ and $UbiV_{Pa}$ was first investigated using transposon (Tn) mutants PW7609 ($ubiT_{Pa}$), PW7610 ($ubiV_{Pa}$), PW7611 ($ubiV_{Pa}$), PW7612 ($ubiU_{Pa}$) and PW7613 ($ubiU_{Pa}$) and the isogenic parental strain MPAO1 (wild-type strain from the Manoil collection) as control (Table S2). Aerobic growth in LB medium was similar between the Tn mutants and the wild-type strain MPAO1 (Fig. 2A) and the mutants presented a UQ_9 level comparable to the wild-type (Fig. 2B). Thus, $UbiT_{Pa}$, $UbiU_{Pa}$ and $UbiV_{Pa}$ are not involved in the O_2-dependent UQ biosynthetic pathway of *P. aeruginosa*. On the contrary, the growth of the $ubiV_{Pa}$ and $ubiU_{Pa}$ mutants was severely impaired in denitrification conditions (Fig. 2C) and their UQ_9 content was strongly diminished (Fig. 2B). These results suggest the overall requirement of $ubiU_{Pa}$ and $ubiV_{Pa}$ for denitrification in *P. aeruginosa*, supposedly *via* their involvement in O_2-independent UQ biosynthesis. Surprisingly, the growth of the $ubiT_{Pa}$ Tn mutant PW7609 was not affected (Fig. 2C) and it showed 40% UQ_9 compared to the wild-type in anaerobic cultures (Fig. 2B). In this mutant, the Tn is inserted at the fifth base of the $ubiT_{Pa}$ gene, potentially leading to only partial inactivation of the gene (Table S2). We note that previous studies with *E. coli ubi* mutants showed that only 20% UQ was sufficient to maintain a wild-type growth phenotype (18,19).

Denitrification is dependent of $ubiT_{Pa}$, $ubiU_{Pa}$ and $ubiV_{Pa}$ genes *via* their involvement in O_2-independent UQ biosynthesis.

As *ubiT*, *ubiV* and *ubiU* are localized next to each other in the genome of PAO1, the transposon inserted in the mutants previously studied might impact the expression of the neighbouring genes. In addition, it is likely that the Tn mutant PW7609 is not disrupting properly the $ubiT_{Pa}$ gene. Thus, we constructed knockout (KO) of the three genes in the parental strain PAO1 and tested their complementation by plasmid-borne genes. The three mutants shared a growth defect under denitrification coupled to a strong decrease of UQ_9 content compared to the wild-type (Fig. 3A and 3B), whereas UQ_9 content and growth were normal in aerobic conditions (Fig. 3B and 3C). We then transformed the mutant strains with an empty vector (pSW196) or the same vector carrying a wild-type allele of the corresponding gene under the control of inducible P_{BAD} promoter. In complemented strains, bacterial growth and UQ_9 levels were restored to the levels of the PAO1 strain used as control (Fig. 4A).

To confirm that UQ was directly involved in the restoration of the anaerobic growth of the *ubiTUV*-KO strains, UQ_4 solubilized in methanol was added to the denitrification medium at 5 and 50 µM final concentrations. After 24h of anaerobic incubation, colony-forming units per mL (CFU/mL) of each KO strain were estimated and compared to the same strain cultivated

without UQ_4. The most significant results were obtained with 50 µM of UQ_4, which increased CFU of KO strains by 8-15 fold (Fig. 4B). We noted a substantial toxicity of methanol on the wild-type strain (Fig. 4B, Ct lane), suggesting that the positive effect of UQ_4 on the KO strains is likely underestimated. Taken together, our results show unequivocally that $UbiT_{Pa}$, $UbiU_{Pa}$ or $UbiV_{Pa}$ are needed for denitrification *via* their involvement in UQ biosynthesis.

$UbiT_{Pa}$, $UbiU_{Pa}$ and $UbiV_{Pa}$ are needed for the process of denitrification.

We used soft-agar experiments to examine dioxygen and nitrate requirements of *ubiT,U,V*-KO strains with or without the wild-type allele. Soft agar was prepared anaerobically in LB medium containing KNO_3 at 100 mM final concentration and then exposed to ambient air. Oxygen diffuses through the agar to form a gradient, the highest concentration being at the top of the agar (Fig. 4C, lane 1). As shown in Fig. 4C, parental strain PAO1 and complemented *ubiTUV*-KO strains grew throughout the tube because they were able to use aerobic respiration as well as denitrification. In contrast, the growth of the *ubiTUV*-KO strains harboring the empty vector was restricted to the oxygenated part of the medium, whereas the presence of the respective genes on the plasmids allowed growth in the anaerobic medium (Fig. 4C). The bubbles observed in the soft agar correspond to gas evolution of N_2O and/or N_2 (12), suggesting a restoration of the denitrification process. Taken together, these results point to the requirement for $ubiT_{Pa}$, $ubiU_{Pa}$ and $ubiV_{Pa}$ beyond the nitrate reduction step and support that UQ is probably essential for the entire denitrification process in *P. aeruginosa*.

Molybdopterin cofactors are not involved in anaerobic UQ_9 biosynthesis.

As mentioned previously, the *ubiUVT* operon is located downstream of the genes *moeA1*, *moaB1*, *moaE*, *moaD* and *moaC* involved in MoCo biosynthesis. Currently MoCo-containing hydroxylases constitute the only family known to catalyze O_2-independent hydroxylation reactions (20). Since three O_2-independent hydroxylation reactions are needed to synthesize UQ anaerobically (9), we reasoned that MoCo might be involved in this process, providing a rationale for the co-localization of the *ubi* and *moa/moe* genes. To test this hypothesis, we evaluated the ability of Tn mutants PW7614, PW7615/PW7616, PW7618/PW2470, PW7619/PW1920 and PW7621/PW7622 (Table S2) corresponding respectively to Tn insertions in the ORFs *moeA1*, *moaB1* (two mutants), *moaE* (two mutants), *moaD* (two mutants) and *moaC* (two mutants) to synthesize UQ_9 without O_2. As expected, all the Tn mutants exhibited a growth defect in denitrification, since MoCo is an essential component of nitrate reductase (17). However, anaerobic growth was rescued by addition of arginine as previously described (21), and we were therefore able to measure the UQ content of the cells in these conditions (Fig. S4). The UQ_9 content of the MoCo Tn mutants was comparable to that of the wild-type strain, suggesting that MoCo is not involved in anaerobic UQ_9 biosynthesis (Fig. S4).

$UbiV_{Pa}$ is an air-sensitive [4Fe-4S] cluster-containing protein.

To gain insights into their biochemical properties, we overproduced and purified the three proteins, $UbiV_{Pa}$ being the most soluble. First, we showed that $UbiV_{Pa}$ purified by size exclusion chromatography (SEC) behaved as a monomer (Fig S5A and S5B). Moreover, the solution of purified $UbiV_{Pa}$ was slightly pink-colored and had a UV-visible absorption spectrum characteristic of the presence of iron-sulfur species (22), with a band at 410 nm and broad and low intensity shoulders between 450 and 600 nm (Fig. 5A, dotted line) (23). However, the amount of iron and sulfur (0.22 iron and 0.22 sulfur/monomer) was largely substoïchiometric, suggesting a degradation of the [Fe-S] cluster during the purification of the protein under aerobiosis, as already observed for many other Fe-S proteins and UbiV protein from *E. coli* (9). Consistent with this hypothesis, anaerobic reconstitution of the [Fe-S] cluster allowed to obtain a brown color protein with a UV-visible spectrum displaying one broad absorption band at 410 nm, which is characteristic of a $[4Fe\text{-}4S]^{2+}$ cluster (Fig. 5A, solid line) (24). The iron and sulfide determination yielded 3.90 ± 0.03 iron and 3.40 ± 0.20 sulfur/monomer of $UbiV_{Pa}$, consistent with the presence of one [4Fe-4S] cluster/protein (Table 1). As shown in Fig S5C, the [Fe-S] cluster of $UbiV_{Pa}$ was sensitive to air.

Four strictly conserved cysteines (C39, C180, C193, and C197) arranged in a $CX_nCX_{12}CX_3C$ motif (X representing any amino acid) are found in $UbiV_{Pa}$ (9). To test if these four cysteines are important for the chelation of the [4Fe-4S] cluster present in $UbiV_{Pa}$, we generated two double

mutants (C193AC197A and C39AC180A) and a triple mutant (C39A, C193A and C197A). All these mutants were colorless after purification and did not show any absorption band in the 350- to -550-nm region of their UV-Vis spectra (Fig. S5D), suggesting that they were impaired in their capacity to accommodate a [Fe-S] cluster. After reconstitution under anaerobic conditions, $UbiV_{Pa}$ C39AC193AC197A precipitated and its UV-vis spectrum could not be recorded. Although they also had a tendency to aggregate, 10% of the double mutants behaved as monomers permitting some assays. Overall, their absorbance at 410 nm (Fig. 5B) and their iron and sulfur contents (Table 1) were largely decreased compared to the wild-type protein, suggesting that the four conserved cysteines are good candidates as ligands of the [4Fe-4S] cluster present in $UbiV_{Pa}$.

Heterologously overproduced $UbiU_{Pa}$ and $UbiT_{Pa}$ co-purify with UQ_8.

We have recently demonstrated that isoprenoid quinones were able to co-elute with the Ubi-proteins such as UbiJ (11) and that UbiT exhibits a sterol carrier protein 2 (SCP2) domain (9). In this direction, we performed lipid content analysis of the $UbiT_{Pa}$, $UbiU_{Pa}$ and $UbiV_{Pa}$ fractions purified from *E. coli* extracts. No isoprenoid quinones were detected co-eluting with $UbiV_{Pa}$ (Table S3). In contrast, UQ_8 and DMQ_8 (2-octaprenyl-3-methyl-6-methoxy-1,4-benzoquinone) were shown to co-purify with $UbiU_{Pa}$. This protein was purified only in the presence of detergent, as it was insoluble without it. After a two-step purification protocol, including a Ni-NTA chromatography and a SEC, the solubilized protein had still a tendency to form different oligomeric states covering the fractions 14 to 44 as shown in Fig.6A and 6B. UQ_8 and DMQ_8 were mainly detected in the elution fractions 33 to 45 (Fig.6A) corresponding to only a proportion of the purified $UbiU_{Pa}$ (Fig.6B). The highest contents, i.e. 488.17 pmoles of UQ_8 per mg of protein and 19 932 AU of DMQ_8 per mg of protein, were assayed in the fraction 39 and 40, respectively (Table S3). This corresponds to a UQ_8/protein ratio of 1.5%. Taken together, these results show that UQ_8 and DMQ_8 co-purify with $UbiU_{Pa}$ depending of its oligomerization state.

Due to a lack of solubility, $UbiT_{Pa}$ was over-produced with *E. coli* thioredoxin (TrxA) as a gene fusion partner, as previously described (25). After the first step of the purification process (Ni-NTA chromatography), the 32 kDa $UbiT_{Pa}$-thioredoxin fusion protein was digested with thrombin. Then in order to remove the thioredoxin His-tagged protein, $UbiT_{Pa}$ was purified by Ni-NTA coupled to SEC, as a high oligomeric form (Fig 6C). The purified $UbiT_{Pa}$ (pool of fractions 20 to 30) contained 9.75±4.57 pmoles of UQ_8 per mg of protein (Fig. 6C and Table S3), which corresponds to a UQ_8/protein ratio of about 0.02%.

$UbiU_{Pa}$ and $UbiT_{Pa}$ bind the isoprenoid tail of UQ.

To further confirm the ability of $UbiT_{Pa}$ and $UbiU_{Pa}$ to bind UQ, a protein–lipid overlay assay was performed (Fig. 6D). We checked the possibility of these proteins to recognize UQ_{10}, UQ_8, solanesol, 3-methylcatechol, 1-palmitoyl-2-oleoyl-*sn*-glycero-3-phosphoethanolamine (POPE) and cholesterol. Solanesol is a non-cyclic terpene alcohol that consists of nine isoprene units as found in UQ_9. 3-methylcatechol was chosen to mimic the head group of UQ. POPE is the major lipid component of the inner membrane of *E. coli* (26). Finally, cholesterol was used as a sterol standard. Fig. 6D shows that $UbiT_{Pa}$, and $UbiU_{Pa}$ did not interact with 3-methylcatechol, POPE, or cholesterol in our experimental conditions. In contrast, both proteins were able to recognize UQ_{10}, UQ_8 and solanesol. We established the ability of $UbiT_{Pa}$ to bind phosphatidic acid (PA) as previously demonstrated by Groenewold *et al*. (25) (Fig. S6). Together, we show that $UbiT_{Pa}$ and $UbiU_{Pa}$ are able to bind the isoprenoid tail of UQ in agreement with their involvement in the O_2-independent biosynthesis pathway of UQ.

DISCUSSION

UQ acts as a membrane-embedded electron and proton shuttle and is a key molecule in the respiratory metabolism of bacteria. Biosynthesis of UQ in aerobic conditions has been widely studied and includes a series of enzymatic reactions in which a benzene ring undergoes a series of modifications (prenylation, decarboxylation, methylation, and hydroxylation). Our chemical analyses identified UQ_9 as the single quinone in the membranes of aerobically grown *P. aeruginosa*, which is in agreement with the literature (7,16). We found in *P. aeruginosa* homologues of the genes known to be involved in UQ biosynthesis, except *ubiF* gene (Table S1). Indeed, as already published, *P. aeruginosa* exhibits a yeast COQ7 protein homologue, which catalyzes the same reaction as UbiF from *E. coli* (15,16). Thereby, both bacteria share a similar UQ biosynthetic pathway

involving three hydroxylases - UbiI, UbiH and UbiF or COQ7 - using O_2 as a co-substrate. As no other isoprenoid quinone was detected in extracts of *P. aeruginosa*, we suppose that UQ_9 is essential for aerobic growth of this bacterium.

In the absence of oxygen, *P. aeruginosa* can grow by dissimilatory nitrate respiration by using nitrate/nitrite as alternative terminal electron acceptors of the respiratory chain. This metabolic process, known as denitrification, has been widely studied (3). However, the component acting to transfer electrons from primary dehydrogenases to nitrate/nitrite reductases was not clearly identified to date (3). In the present study, we identified UQ_9 as the single quinone synthesized in anaerobic conditions, suggesting that *P. aeruginosa* possesses an O_2-independent UQ biosynthetic pathway. We recently identified such pathway in *E. coli* (9) and here we characterized three genes, *ubiT*$_{PA}$ *(PA3911)*, *ubiU*$_{PA}$ *(PA3913)* and *ubiV*$_{PA}$ *(PA3912)*, which are essential for the anaerobic UQ biosynthesis pathway and are dispensable for the aerobic one. *E. coli* grows normally in anaerobiosis in a UQ-independent manner because of the presence of naphthoquinones (9) (27) (28). In contrast, we demonstrated that these three genes were essential to anaerobic denitrification metabolism of *P. aeruginosa*, which is in agreement with the presence of a single quinone organism, in this case UQ. Interestingly, *ubiV*$_{Pa}$ (*PA3912*) and *ubiU*$_{Pa}$ (*PA3913*) are expressed in response to anaerobic conditions (29) and abundance of $UbiU_{Pa}$ protein was increased during anaerobic growth (30). Moreover, using random transposon mutagenesis, *ubiV*$_{Pa}$ (*PA3912*) and *ubiU*$_{Pa}$ (*PA3913*) were already reported as essential for anaerobic growth of *P. aeruginosa* on nitrate, nitrite and arginine (21).

Although its contribution is still poorly understood in the host, anaerobic respiration of *P. aeruginosa* is likely significant to promote virulence mechanisms in chronic lung infections (13). Indeed, according to O_2 assays directly in the lungs of CF patients, the infected endobronchial mucus is subject to severe hypoxia or even anoxia (31). Two hypotheses were proposed to explain this phenomenon in the literature. First, it may be due to the biofilm structure *per se* may establish an oxygen gradient across. However, this hypothesis is currently questioned due to the strong morphological differences between *in vivo* and *in vitro* biofilm production, the last being much more thicker than the first, for example (13). The second hypothesis is that accelerated O_2 consumption in the biofilm may result from activated polymorphonuclear leukocytes that produce superoxide (32) and to a lesser extend nitric oxide (33). Additional host responses also affect the availability of alternative electron acceptors for anaerobic bacterial metabolism. For example, high levels of nitrate and nitrite have been measured in CF sputum of patients (34). From all these observations and as UQ is an essential component acting to transfer electrons from primary dehydrogenases to reductases in *P. aeruginosa* in anaerobic conditions, we propose that UbiT, UbiV and UbiU may contribute to the CF lung infection (work in progress in our laboratory). This hypothesis is supported by a recent quantitative proteomics approach revealing increased abundance of $UbiT_{Pa}$, $UbiU_{Pa}$ and $UbiV_{Pa}$ in anaerobic biofilm (25). Moreover, deduced from a high-throughput sequencing of Tn libraries from *P. aeruginosa* strain PA14, it appears that *ubiA*, *ubiB*, *ubiC*, *ubiE* or *ubiT* genes are essential for this bacterium to colonize the murine gastrointestinal tract (36). O_2-dependent and O_2-independent UQ biosynthetic pathways share the proteins UbiA, UbiB, UbiC and UbiE (9). However, UbiT is only required under anaerobic conditions (9 and this work), which suggests that O_2-independent UQ biosynthesis would be essential for virulence. This hypothesis is supported by the contribution of UbiU and UbiV paralogs to *Yersinia ruckeri* virulence (37).

In order to better understand their role, we decided to overproduce, purify and biochemically characterize $UbiT_{Pa}$, $UbiU_{Pa}$ and $UbiV_{Pa}$. Our results showed that $UbiV_{Pa}$ is an air-sensitive Fe-S containing protein, like UbiV from *E.coli* (9), and we demonstrated that cysteines 39, 180, 193 and 197 are ligands to the [4Fe-4S] cluster found in $UbiV_{Pa}$. From these results, we confirm the conservation in homologs of UbiV of a four cysteines pattern coordinating a Fe-S cluster common to RlhA and TrhP, which belong to the same family of protein, i.e. the proteases U32, and which are also involved in O_2-independent hydroxylations (38,39). However, the exact roles of UbiV and UbiU in the hydroxylation steps remains to be understood. Especially, the role of the iron-sulfur center of UbiV will have to be investigated. $UbiU_{Pa}$ is a unstable protein. Unlike UbiU from *E. coli*, which forms a stable heterodimer UbiU-UbiV complex (9), we were not able to solubilize $UbiU_{Pa}$ by co-producing it with its potential partner $UbiV_{Pa}$. The fact that we are producing *P. aeruginosa* proteins in *E.coli* could explain this difference of behavior. In any

case, an UbiU-UbiV complex in *P. aeruginosa* is a reasonable hypothesis that still needs to be demonstrated. Moreover, in contrast to UbiU from *E. coli*, we were able to purify $UbiU_{Pa}$ alone with significant quantities of UQ_8 and DMQ_8, whereas purified $UbiV_{Pa}$ contained no quinones. This result was confirmed by a protein-lipid overlay assay, which showed that the isoprenoid tail was the structural determinant for the recognition by $UbiU_{Pa}$. From theses results, we can propose that UbiU would bind the lipidic intermediates of the anaerobic UQ pathway. UbiT contains a SCP2 domain similar to that of UbiJ (40) and a previous study showed that PA3911 ($UbiT_{Pa}$) was able to bind specifically PA, the central hub of phospholipid metabolism (25). This result was confirmed (Fig. S6) and we showed that $UbiT_{Pa}$ co-purifies also with UQ_8. This result supports the hypothesis that UbiT may be the counterpart of UbiJ in anaerobic conditions, binding UQ intermediates and stabilizing a putative Ubi complex, functions that have yet to be demonstrated.

EXPERIMENTAL PROCEDURES

Bacterial strains and growth conditions.

P. aeruginosa and *E. coli* strains used in this study are listed in Table S2. We obtained the collection of transposon (Tn) mutants in *P. aeruginosa* MPAO1 strain from the Manoil Laboratory, Department of Genome Science, University of Washington, USA (41,42). The Tn insertion site of the mutant strains were verified by sequencing (GATC Biotech, Konstanz, Germany) using PCR primers recommended by the library curators. *P. aeruginosa* strains were aerobically maintained at 37°C on lysogeny broth (LB) agar plates. For quinone assay, aerobic cultures (5 mL) were performed in LB medium at 37°C with rotary shaking at 200 rpm. Anaerobic growth of *P. aeruginosa* were performed in a 12 mL Hungate tubes containing LB medium supplemented with KNO_3 as an electron acceptor (100 mM final concentration) (43), hereafter called denitrification medium, and deoxygenated 30 min by argon bubbling (O_2<0.1 ppm) prior to autoclaving. In some experiments, LB medium was supplemented with arginine at a final concentration of 40 mM instead of KNO_3 (44). Hungate tubes were inoculated through the septum with 100 µL of overnight cultures taken with disposable syringe and needles from closed Eppendorf tubes filled to the top. Cultures in hungate tubes were used for measuring the quinone contents. For aerobic growth studies, aerobic overnight cultures were used to inoculate a 96-well plate to obtain a starting optical density at 600 nm (OD_{600}) of 0.05 and further incubated with shaking at 37°C. Changes in OD_{600} were monitored every 10 min for 12 h using the Infinite 200 PRO microplate reader (Tecan, Lyon, France). For anaerobic growth curve studies, overnight cultures in 50 mL closed tubes of not degassed denitrification medium were used to inoculate 400 mL bottles to obtain a starting OD_{600} of 0.05. Then, bacteria were grown anaerobically by sparging argon (O_2<0.1 ppm) and bacterial cultures were monitored spectrophotometrically (OD_{600}) at 30 min intervals. *E. coli* MG1655 and DH5α were grown on LB agar or in LB liquid. When required, the medium was supplemented with ampicillin at 100 µg/ml for *E. coli*, carbenicillin at 250 µg/ml for *P. aeruginosa*, or tetracycline at 60 µg/ml for *E. coli* and 100 µg/ml for *P. aeruginosa* or gentamicin at 200 µg/mL for *P. aeruginosa* (Table S2). When necessary, UQ_4 or 0.1% (w/v) arabinose final concentration was added to the medium to enhance bacterial anaerobic growth or to induce P_{BAD} expression of pSW196-derived plasmids, respectively. *Pseudomonas* Isolation Agar (PIA) medium (from DB) containing irgasan (25 µg/L) was used for triparental mating to counter select *E. coli*. For CFU counting, bacteria were suspended in PBS and cell suspensions were serially diluted in PBS. For each sample, 100 µL of at least four different dilutions were plated on LB plates, incubated for 24h at 37°C and CFU were counted using a Scan 100 Interscience.

Plasmids and genetic manipulations.

The plasmids and the primers used in this study are listed in Tables S2 and S4). All the plasmids produced in this work were checked using DNA sequencing (GATC Biotech, Konstanz, Germany). To generate *P. aeruginosa* deletion mutants, overlapping upstream and downstream flanking regions of $ubiT_{Pa}$, $ubiU_{Pa}$ and $UbiV_{Pa}$ genes were obtained by PCR amplification using PAO1 genome as template and the oligonucleotides described in Table S4. The resulting fragments were then cloned into *Sma*I-cut pEXG2 plasmid by sequence and ligation-independent cloning (45). To complement the mutants, the $ubiT_{Pa}$, $ubiU_{Pa}$ and $ubiV_{Pa}$ fragments were generated by PCR amplification using the oligonucleotide pairs ubiT-PA-F/ubiT-PA-R, ubiU-PA-F/ubiU-PA-R and ubiV-PA-F/ubiV-PA-R, respectively, and

PAO1 genome as template (Table S4). The fragments were *Eco*RI-*Sac*I digested and inserted into P_{BAD}-harboring pSW196 plasmid, yielding the p*ubiT*$_{Pa}$, p*ubiU*$_{Pa}$ and p*ubiV*$_{Pa}$ plasmids, respectively (Table S2). The pEXG2- and pSW196-derived vectors were transferred into *P. aeruginosa* PAO1 strain by triparental mating using pRK2013 as a helper plasmid (46). For allelic exchange using the pEXG2 plasmids, co-integration events were selected on PIA (*Pseudomonas* Isolation Agar) plates containing gentamicin. Single colonies were then cultured on NaCl-free LB agar plates containing 10% (w/vol) sucrose to select for the loss of the plasmid, and the resulting sucrose-resistant colonies were checked for mutant genotype by PCR. To overproduce C-terminally His-tagged UbiV$_{Pa}$, the *ubiV*$_{Pa}$ gene was cloned into the pET22b(+) vector. The *ubiV*$_{Pa}$ insert was obtained by PCR amplification using the oligonucleotide pair (pET22b-UbiV$_{Pa}$-F and pET22-UbiV$_{Pa}$-R and *ubiV*$_{Pa}$ ORF as template (Table S4). *Nde*I-*Xho*I digested amplicon was ligated to *Nde*I-*Xho*I digested pET22b(+) vector to obtain pET22-UbiV$_{Pa}$ (Table S2). Variants of UbiV$_{Pa}$ were obtained using the Q5 Site-Directed Mutagenesis Kit (New England Biolabs) (UbiV$_{Pa}$ C193AC197A and UbiV$_{Pa}$ C39AC193AC197A) and the QuickChange II XL Site-Directed Mutagenesis Kit (Agilent) (UbiV$_{Pa}$ C39AC180A) according to the manufacturer's specifications using pET22b-UbiV$_{Pa}$ as template (Table S2 and S4).

Soft-agar study to evaluate the O_2-dependency of growth.

Soft-agar studies were performed in denitrification medium supplemented by agar 0.7% (w/v) final concentration. After argon bubbling (O_2<0.1 ppm) for 30 min, the suspension (13 mL) was autoclaved in Hungate tubes. They were then placed in a 40°C incubator and they were inoculated through the septum with 100 µL of overnight cultures taken with disposable syringe and needles from Eppendorf tubes filled to the top, mixed by inverting, and incubated at room temperature 30 min to allow the agar to solidify. Then, the tubes were incubated under aerobic conditions with caps loosened at 37°C for 24h. A control experiment was performed with resazurin (0.25 µg/mL final concentration) used as an indicator of medium oxygenation. When required, the medium was supplemented with antibiotics.

Lipid extractions and quinone analysis.

Cultures (5 mL under ambient air and 13 mL under anaerobic conditions) were cooled down on ice before centrifugation at 3200 g, 4°C, 10 min. Cell pellets were washed in 1 mL ice-cold PBS and transferred to pre-weighted 1.5 mL Eppendorf tubes. After centrifugation at 12000 g, 4°C, 1 min and elimination of supernatant, the cell wet weight was determined (~5-30 mg) and pellets were stored at -20°C. Quinone extraction from cell pellets was performed as previously described (18). Lipid extracts corresponding to 1 mg of cell wet weight were analyzed by HPLC electrochemical detection-mass spectrometry (ECD-MS) with a BetaBasic-18 column at a flow rate of 1 mL/min with mobile phases composed of methanol, ethanol and a mix of 90% isopropanol, 10% ammonium acetate (1 M), 0.1% TFA: mobile phase 1 (50% methanol, 40% ethanol and 10% mix). When necessary, MS detection was performed on a MSQ spectrometer (Thermo Scientific) with electrospray ionization in positive mode (probe temperature 400°C, cone voltage 80V). Single ion monitoring (SIM) detected the following compounds: UQ_8 ($M+NH_4^+$), m/z 744-745, 6-10 min, scan time 0.2 s; UQ_9 ($M+NH_4^+$), m/z 812-813, 9-14 min, scan time 0.2 s; UQ_{10} ($M+NH_4^+$), m/z 880.2-881.2, 10-17 min, scan time 0.2 s., DMQ_8 ($M+NH_4^+$), m/z 714-715, 5-10 min, scan time 0.2 s. MS spectra were recorded between m/z 600 and 900 with a scan time of 0.3 s. ECD and MS peak areas were corrected for sample loss during extraction on the basis of the recovery of the UQ_{10} internal standard and were then normalized to cell wet weight. The peaks of UQ_8 and UQ_9 obtained with electrochemical detection were quantified with a standard curve of UQ_{10} as previously described (18).

Overproduction and purification of UbiV, UbiU and UbiT from *Pseudomonas aeruginosa*.

Wild-type and variants UbiV$_{Pa}$ were expressed and purified as previously described for E. coli proteins (9). Briefly, the pET-22b(+) plasmid, encoding wild-type or variants UbiV, were co-transformed with pGro7 plasmid (Takara Bio Inc.) into *E. coli* BL21 (DE3) Δ*ubiUV* competent cells grown at 37 °C in LB medium, which was supplemented with ampicillin (50 µg/mL), kanamycin (50 µg/mL) and chloramphenicol (12.5 µg/mL). At an OD_{600} = 1.2, D-arabinose was added to the cultures at a final concentration of 2 mg/mL. At an OD_{600} = 1.8, cultures were cooled down on ice for 20 min, and IPTG was added at a final concentration of 0.1 mM. Cells were then

allowed to grow further at 16 °C overnight. Wild-type $UbiV_{Pa}$ and the different variants were purified by Ni-NTA affinity chromatography followed by SEC in buffer A (50 mM Tris-HCl, 25 mM NaCl, 15% (v/v) glycerol, pH 8.5) containing 1 mM DTT. The purified proteins were concentrated to 30-40 mg/mL using Amicon concentrators (30-kDa cutoff; Millipore).

The overproduction of wild-type $UbiU_{Pa}$ was performed in *E. coli* BL21 (DE3) Δ*ubiU-ubiV* cells by following the same protocol as that for $UbiV_{Pa}$, except that $ubiU_{Pa}$ over-expression was induced with 0.05 mM of IPTG and the cell pellets were resuspended in buffer B (50 mM Tris-HCl, 500 mM NaCl, 15% (v/v) glycerol, pH 8.5) containing 0.2% (m/v) N-lauroylsarcosine sodium salt. After cell disruption by sonication, the clarified cell-free extracts were loaded onto a His-Trap FF crude column (GE Healthcare) pre-equilibrated with buffer B containing 0.1% (m/v) N-lauroylsarcosine sodium salt. The column was washed with 10 column volumes of buffer C (50 mM Tris-HCl, 500 mM NaCl, 15% (v/v) glycerol, 10 mM imidazole, pH 8.5) containing 6 mM N,N-dimethyldodecylamine N-oxide (LDAO) to remove non-specifically bound *E. coli* proteins and then eluted with a linear gradient of 10 column volumes of buffer C containing 500 mM imidazole and 6 mM LDAO. Fractions containing $UbiU_{Pa}$ were pooled and then loaded on a HiLoad 16/600 Superdex 200 pg (GE Healthcare) pre-equilibrated in buffer D (50 mM Tris-HCl, 150 mM NaCl, 15% (v/v) glycerol, pH 8.5) containing 3 mM LDAO. For protein-lipid overlay, fraction 34-43 were pooled and were concentrated using Amicon concentrators (30-kDa cutoff; Millipore), aliquoted, frozen in liquid nitrogen, and stored at -80°C.

Overproduction of $UbiT_{Pa}$ fused with the thioredoxin (Trx-$UbiT_{Pa}$) in *E. coli* BL21 (DE3) Δ*ubiU-ubiV* cells was performed by following the same protocol as that for $UbiU_{Pa}$, except that over-expression of chimeric gene was induced at an OD_{600} of 0.5 and the cell pellet was resuspended in buffer B containing 5% (w/v) sodium cholate. Trx-$UbiT_{Pa}$ was first purified, following the same protocol as that for $UbiU_{PA}$, by Ni-NTA chromatography, except that the buffers C and D contained 0.5% (m/v) sodium cholate. Fractions containing Trx-$UbiT_{Pa}$ were pooled and detergent was removed using a Hiprep 26/10 Desalting column (GE Healthcare) preequilibrated with buffer E (50 mM Tris-HCl, 150 mM NaCl, 15% (v/v) glycerol, pH 8.5). The fusion protein was digested with thrombin (10 units/mg of Trx-$UbiT_{Pa}$) at room temperature and then loaded on a HiLoad 16/600 Superdex 200 pg (GE Healthcare) coupled with a HisTrap FF crude column (GE Healthcare) pre-equilibrated in buffer E. The purified proteins were concentrated using Amicon concentrators (100-kDa cutoff; Millipore), aliquoted, frozen in liquid nitrogen, and stored at -80°C.

[Fe-S] cluster reconstitution.

The [Fe-S] cluster(s) of holo-$UbiV_{Pa}$ and holo-variants were reconstituted as previously described (9). Briefly, a solution containing 100 µM of as-purified proteins was treated with 5 mM DTT for 15 min at 20°C and then incubated for 1 h with a 5-fold molar excess of both ferrous ammonium sulfate and L-cysteine. The reaction was initiated by the addition of a catalytic amount of the *E. coli* cysteine desulfurase CsdA (1-2% molar equivalent) and monitored by UV-visible absorption spectroscopy. After 1 h of incubation, the holo-proteins were then loaded onto a Superdex 75 Increase 10/300 GL column (GE Healthcare) pre-equilibrated with buffer A. The fractions containing the holo-proteins were pooled and concentrated to 20-30 mg/mL on a Vivaspin concentrator (30-kDa cutoff).

Protein–lipid overlay.

To assess the lipid-binding properties of $UbiT_{Pa}$ and $UbiU_{Pa}$, a protein–lipid overlay was performed as previously described (47). Briefly, 2 µL of 20 mM lipids in dichloromethane were spotted onto PVDF membrane and allowed to dry at room temperature for 1 h. The membrane was blocked in 3 % (w/v) fatty acid-free BSA in TBST (50 mM Tris-HCl, , 150 mM NaCl and 0.1% (v/v) Tween-20, pH 7.5) for 1 h. The membrane was then incubated overnight at 4 °C in the same solution containing 0.2 µg/mL of the indicated proteins. After washing, the membrane was incubated for 1 h with a 1/1.000 dilution of anti-polyHis monoclonal antibody (Sigma) and then for 1 h with a 1/10.000 dilution of anti-mouse–horseradish peroxidase conjugate (Thermo Fisher Scientific). His-tagged proteins bound to the membrane by virtue of its interaction with lipid, were detected by enhanced chemiluminescence.

Quantification Methods.

Protein concentrations were determined using the method of Bradford (Bio-Rad) with bovine serum albumin as the standard. The iron and acid-labile sulfide were determined according to the method of Fish (48) and Beinert (49),

respectively, before and after [4Fe-4S] cluster reconstitution.

UV-vis spectroscopy.

UV-visible spectra were recorded in 1-cm optic path quartz cuvettes under aerobic conditions on a Cary 100 Uv-vis spectrophotometer (Agilent) and under anaerobic conditions in a glove box on a XL-100 Uvikon spectrophotometer equipped with optical fibers.

The abbreviations used are: MK, menaquinone; UQ, ubiquinone; DMK, dimethyl-menaquinone; DMQ, 2-octaprenyl-3-methyl-6-methoxy-1,4-benzoquinone; SEC, size exclusion chromatography; SCP, sterol carrier protein; IPTG, isopropyl-1-thio-β-D-galactopyranoside; ECD, electrochemical detection; PA: phosphatidic acid; POPE: 3-methylcatechol, 1-palmitoyl-2-oleoyl-*sn*-glycero-3-phosphoethanolamine

Author contributions: L. P., F. B., M. F., M. L. conceived and designed the experiments. C. -D. -T., J. M., S. E., E. B., and L. P. performed the experiments. E. B. and B. F. contributed reagents/materials/analysis tools. L. P., M. L., and F. P. wrote the paper. All authors analyzed the results and approved the final version of the manuscript.

ACKNOWLEDGEMENTS

This work was supported by the Agence Nationale de la Recherche (ANR), projects (An)aeroUbi ANR-15-CE11-0001-02, O_2-taboo ANR-19-CE44-0014, DYNAMO ANR-11-LABX-0011-01 and ANR-10-LABX-62-IBEID, the University Grenoble Alpes (UGA), the French Centre National de la Recherche Scientifique (CNRS) and the Commissariat à l'Energie Atomique et aux Energies Alternatives (CEA)

COMPETING INTERESTS

The authors declare that they have no competing interests.

LEGENDS

Figure 1: UQ_9 is the single quinone used by *P. aeruginosa* in aerobic and anaerobic conditions. HPLC-ECD analysis of lipid extracts from 1 mg of cells after growth of *E. coli* MG1655 (E. c.) and *P. aeruginosa* PAO1 (P. a.) aerobically in LB medium **(A)** or anaerobically in LB medium supplemented with 100 mM nitrate **(B)**. The chromatograms are representative of three independent experiments. The peaks corresponding to UQ_8, UQ_9, demethylmenaquinone (DMK_8), menaquinone (MK_8) and the UQ_{10} standard are indicated. **(C)** Mass spectrum of the quinone eluting at 11.5 min from extracts of *P. aeruginosa* grown in aerobic and anaerobic cultures.

Figure 2: UQ_9 content is impaired in the $ubiU_{Pa}$, $ubiV_{Pa}$ and $ubiT_{Pa}$ Tn mutants during denitrification. Representative growth curves of wild-type MPAO1 and Tn mutants grown aerobically in LB medium **(A)** or anaerobically in denitrification medium **(C)**. Data are representative of three independent experiments. **(B)** Quantification of cellular UQ_9 content (n=3) in lipid extracts from wild-type MPAO1 and Tn mutants cells grown aerobically in LB medium (white bars) or anaerobically in denitrification medium (grey bars). Error bars represent S.D.

Figure 3: $ubiU_{Pa}$, $ubiV_{Pa}$ and $ubiT_{Pa}$ are essential for anaerobic UQ_9 biosynthesis and for denitrification. Representative growth curves of wild-type PAO1 and KO for the genes $ubiU_{Pa}$, $ubiV_{Pa}$ and $ubiT_{Pa}$ grown **(A)** in denitrification medium or **(C)** aerobically in LB medium. **(B)** Quantification of cellular UQ_9 content (n=3) in lipid extracts from wild-type PAO1 and KO cells grown aerobically in LB medium (white bars) or in denitrification medium (grey bars). Error bars represent S.D.

Figure 4: Complementation of Ubi KO restores bacterial growth over the entire O_2 range in a UQ-dependent manner. (A) Photographs of culture tubes after overnight growth under anaerobic conditions in denitrification medium of *ΔubiTUV* strains transformed with the empty vector pSW196 or the same vector carrying the corresponding wild-type allele ($ubiT_{Pa}$, $ubiU_{Pa}$ and $ubiV_{Pa}$). The parental strain PAO1 was used as a control and UQ_9 content of wild-type and Δ*ubi* strains cultured anaerobically (n=3) was assayed. **(B)** *ΔubiUVT* strains were cultured in denitrification medium supplemented with methanol-

solubilized UQ_4 at 5 or 50 µM final concentration. After 24h of incubation, colony-forming units per mL (CFU/mL) of each KO strain were estimated and compared to the same strain grown without UQ_4. As a control, toxicity of methanol was tested on the parental strain grown in the same medium but supplemented with 4.5% (v/v) methanol (Ct), which is the final concentration of methanol corresponding to the adding of 50 µM of UQ_4. **(C)** As in **(A)** but in soft-agar tubes after overnight culture. All the strains studied were inoculated into anaerobic tubes and then exposed to ambient air to create an oxygen gradient. The controls (Ct) correspond to soft agar tubes supplemented with 2.5 µg/mL resazurin and then incubated with (1) or without air (2). Oxic and anoxic parts of the agar are indicated. For all strains containing pSW196 vectors, denitrification medium was also supplemented with 0.1% (w/v) final concentration of arabinose to induce P_{BAD} promoter.

Figure 5: $UbiU_{Pa}$ is a [4Fe-4S] containing enzyme. (A) UV-visible absorption of as-purified $UbiU_{Pa}$ (dotted line, 32.6 µM) and reconstituted holo-$UbiU_{Pa}$ (solid line, 22.7 µM). The inset is an enlargement of the 300 to 800 nm region. The molar extinction coefficient, ε_{410nm} was determined to be 12.95 ± 0.5 mM^{-1} cm^{-1} for holo-$UbiV_{Pa}$. **(B)** Comparative UV-visible absorption spectra of wild-type and different Cys-to-Ala mutants of $UbiV_{Pa}$ after metal cluster reconstitution. Proteins were analyzed at the following concentrations: 22.7µM WT, 34.8 µM C39A C180A and 15.9 µM C193A C197A. Proteins were suspended in buffer 50 mM Tris-HCl, 25 mM NaCl, 15% (v/v) glycerol, 1 mM DTT, pH 8.5.

Figure 6: $UbiU_{Pa}$ and $UbiT_{Pa}$ bind UQ_8. (A) Elution profile of $UbiU_{Pa}$, 70 mg of protein were loaded on a Superdex 200 16/60 chromatography column. A quantification of UQ_8 and DMQ_8 in each fraction was performed by HPLC-ECD MS. A recovery of 73 and 76%, respectively for UQ_8 and DMQ_8, was calculated from the total content of all fractions compared with content of the $UbiU_{PA}$ purified fraction deposited on the Superdex 200 column. **(B)** Fractions 10 to 44 analyzed by SDS-PAGE for purity. **(C)** Elution profile of $UbiT_{Pa}$ on a Superdex 200 16/60 column. Inset, SDS-PAGE, lane 1, 32 kDa $UbiT_{Pa}$-TrxA fusion protein, lane 2, after digestion with thrombin (UbiT, 19.6kDa and TrxA, 12.1 kDa), lane 3, pooled fractions 20-30 of $UbiT_{Pa}$. Quantification of UQ_8 (pool of fractions 20 to 30) was performed by HPLC-ECD MS **(D)** Protein-lipid overlay assay between $UbiU_{Pa}$ and $UbiT_{Pa}$ and different lipid ligands. 2 µL of six different lipid/compound potential candidates (1, UQ_8; 2, UQ_{10}; 3, solanesol; 4, 3-methylcatechol; 5, cholesterol; 6, POPE) at 20 mM final concentration were spotted on a PVDF membrane and then incubated with $UbiT_{Pa}$ or $UbiU_{Pa}$ (both proteins at 0.2 µg/mL final concentration). Detection of bound proteins was performed by chemiluminescence, as described in Experimental Procedures section.

Figure S1: Zoom (740 to 840 m/z region) of the mass spectrum displayed in Fig. 1C. H^+, NH_4^+ and Na^+ adducts corresponding to UQ_9 were indicated.

Figure S2: Putative UQ_9 biosynthetic pathways in *E. coli* MG1655 and in *P. aeruginosa* PAO1. Proteins common to both biosynthetic pathways (aerobic and anaerobic) are indicated in black. Proteins involved only in aerobiosis or in anaerobiosis are indicated in red or in blue, respectively. The function of UbiT, UbiU and UbiV remains unclear. Corresponding gene IDs in *P. aeruginosa* are indicated in parenthesis. UbiF is only identified in *E. coli* and its functional homolog *in P. aeruginosa* is a Coq7-like hydroxylase.

Figure S3: Genomic localization of the *ubiUVT* operon in from *P. aeruginosa* PAO1. ORFs of $ubiT_{Pa}$, $ubiU_{Pa}$ and $ubiV_{Pa}$ genes are represented by green, blue and orange arrow, respectively.

Figure S4: Molybdopterin cofactors are not involved in anaerobic biosynthesis of UQ_9 in *P. aeruginosa*. Quantification of cellular UQ_9 content (n=3) in lipid extracts from wild-type MPAO1 and Tn mutants cells (see Table S2) grown overnight anaerobically in LB medium supplemented with arginine. Error bars are means ± S.D. Anaerobic growth of wild-type and Tn mutants was assessed in denitrification medium or in LB supplemented with arginine (40 mM final concentration) after 48h of incubation. (+), growth; (-) no growth.

Figure S5: (A) Gel filtration chromatogram of aerobically purified $UbiV_{Pa}$ on a Superdex 75 Increase 10/300 GL column; Inset: SDS-PAGE of purified $UbiV_{Pa}$. **(B)** Calibration curve, standard proteins in rhombi, $UbiV_{Pa}$ in circle. **(C)** UV-visible absorption spectra of 22.7 µM holo-$UbiV_{Pa}$ under anaerobiosis (solid line) and after 30 min exposure to air (dotted line). **(D)** Comparative UV-visible absorption spectra of aerobically purified wild-type (black) and various Cys-to-Ala mutants of $UbiV_{Pa}$ (C39A C180A in red; C193AC197A in blue; C39AC193AC197A in green). Inset: enlargement of the 300 to 800 nm region and Coomassie staining SDS-PAGE showing the purifications of WT-$UbiV_{Pa}$ and its variants. Lanes: M, molecular weight marker; 1, wild-type $UbiV_{Pa}$; 2, $UbiV_{Pa}$ C39A C180A; 3, $UbiV_{Pa}$ C193A C197A; 4, $UbiV_{Pa}$ C39A C193A C197A. All proteins were suspended in 50 mM Tris-HCl, 25 mM NaCl, 15% (v/v) glycerol, 1 mM DTT, pH 8.5.

Figure S6: Protein-Lipid Overlay assay between $UbiT_{Pa}$ and phosphatidic acid (PA). 2 µL of four different lipid/compound (1, 3-methylcatechol; 2, POPE; 3, UQ_{10} and 4, cholesterol) at 20 mM final concentration were spotted on a PVDF membrane and then incubated with $UbiT_{Pa}$ at 0.2 µg/mL final concentration. Detection of bound protein was performed by chemiluminescence, as described in Experimental Procedures section.

REFERENCES

1. Crull, M. R., Somayaji, R., Ramos, K. J., Caldwell, E., Mayer-Hamblett, N., Aitken, M. L., Nichols, D. P., Rowhani-Rahbar, A., and Goss, C. H. (2018) Changing Rates of Chronic Pseudomonas aeruginosa Infections in Cystic Fibrosis: A Population-Based Cohort Study. *Clin Infect Dis* **67**, 1089-1095
2. Magill, S. S., Edwards, J. R., Bamberg, W., Beldavs, Z. G., Dumyati, G., Kainer, M. A., Lynfield, R., Maloney, M., McAllister-Hollod, L., Nadle, J., Ray, S. M., Thompson, D. L., Wilson, L. E., Fridkin, S. K., Emerging Infections Program Healthcare-Associated, I., and Antimicrobial Use Prevalence Survey, T. (2014) Multistate point-prevalence survey of health care-associated infections. *N Engl J Med* **370**, 1198-1208
3. Arai, H. (2011) Regulation and Function of Versatile Aerobic and Anaerobic Respiratory Metabolism in *Pseudomonas aeruginosa*. *Front Microbiol* **2**, 103
4. Williams, H. D., Zlosnik, J. E., and Ryall, B. (2007) Oxygen, cyanide and energy generation in the cystic fibrosis pathogen *Pseudomonas aeruginosa*. *Adv Microb Physiol* **52**, 1-71
5. Torres, A., Kasturiarachi, N., DuPont, M., Cooper, V. S., Bomberger, J., and Zemke, A. (2019) NADH Dehydrogenases in *Pseudomonas aeruginosa* Growth and Virulence. *Front Microbiol* **10**, 75
6. Page, A. C., Jr., Gale, P., Wallick, H., Walton, R. B., Mc, D. L., Woodruff, H. B., and Folkers, K. (1960) Coenzyme Q. 17. Isolation of coenzyme Q10 from bacterial fermentation. *Arch Biochem Biophys* **89**, 318-321
7. Matsushita, K., Yamada, M., Shinagawa, E., Adachi, O., and Ameyama, M. (1980) Function of ubiquinone in the electron transport system of *Pseudomonas aeruginosa* grown aerobically. *J Biochem* **88**, 757-764
8. Nowicka, B., and Kruk, J. (2010) Occurrence, biosynthesis and function of isoprenoid quinones. *Biochim Biophys Acta* **1797**, 1587-1605
9. Pelosi, L., Vo, C. D., Abby, S. S., Loiseau, L., Rascalou, B., Hajj Chehade, M., Faivre, B., Gousse, M., Chenal, C., Touati, N., Binet, L., Cornu, D., Fyfe, C. D., Fontecave, M., Barras, F., Lombard, M., and Pierrel, F. (2019) Ubiquinone Biosynthesis over the Entire O2 Range: Characterization of a Conserved O2-Independent Pathway. *mBio* **10**
10. Alexander, K., and Young, I. G. (1978) Alternative hydroxylases for the aerobic and anaerobic biosynthesis of ubiquinone in *Escherichia coli*. *Biochemistry* **17**, 4750-4755
11. Hajj Chehade, M., Pelosi, L., Fyfe, C. D., Loiseau, L., Rascalou, B., Brugiere, S., Kazemzadeh, K., Vo, C. D., Ciccone, L., Aussel, L., Coute, Y., Fontecave, M., Barras, F., Lombard, M., and Pierrel, F. (2019) A Soluble Metabolon Synthesizes the Isoprenoid Lipid Ubiquinone. *Cell Chem Biol* **26**, 482-492 e487

12. Zumft, W. G. (1997) Cell biology and molecular basis of denitrification. *Microbiol Mol Biol Rev* **61**, 533-616
13. Jensen, P. O., Kolpen, M., Kragh, K. N., and Kuhl, M. (2017) Microenvironmental characteristics and physiology of biofilms in chronic infections of CF patients are strongly affected by the host immune response. *APMIS* **125**, 276-288
14. Borrero-de Acuna, J. M., Timmis, K. N., Jahn, M., and Jahn, D. (2017) Protein complex formation during denitrification by *Pseudomonas aeruginosa*. *Microb Biotechnol* **10**, 1523-1534
15. Stenmark, P., Grunler, J., Mattsson, J., Sindelar, P. J., Nordlund, P., and Berthold, D. A. (2001) A new member of the family of di-iron carboxylate proteins. Coq7 (clk-1), a membrane-bound hydroxylase involved in ubiquinone biosynthesis. *J Biol Chem* **276**, 33297-33300
16. Jiang, H. X., Wang, J., Zhou, L., Jin, Z. J., Cao, X. Q., Liu, H., Chen, H. F., and He, Y. W. (2019) Coenzyme Q biosynthesis in the biopesticide Shenqinmycin-producing *Pseudomonas aeruginosa* strain M18. *J Ind Microbiol Biotechnol*
17. Coelho, C., and Romao, M. J. (2015) Structural and mechanistic insights on nitrate reductases. *Protein Sci* **24**, 1901-1911
18. Hajj Chehade, M., Loiseau, L., Lombard, M., Pecqueur, L., Ismail, A., Smadja, M., Golinelli-Pimpaneau, B., Mellot-Draznieks, C., Hamelin, O., Aussel, L., Kieffer-Jaquinod, S., Labessan, N., Barras, F., Fontecave, M., and Pierrel, F. (2013) ubiI, a new gene in *Escherichia coli* coenzyme Q biosynthesis, is involved in aerobic C5-hydroxylation. *J Biol Chem* **288**, 20085-20092
19. Loiseau, L., Fyfe, C., Aussel, L., Hajj Chehade, M., Hernandez, S. B., Faivre, B., Hamdane, D., Mellot-Draznieks, C., Rascalou, B., Pelosi, L., Velours, C., Cornu, D., Lombard, M., Casadesus, J., Pierrel, F., Fontecave, M., and Barras, F. (2017) The UbiK protein is an accessory factor necessary for bacterial ubiquinone (UQ) biosynthesis and forms a complex with the UQ biogenesis factor UbiJ. *J Biol Chem* **292**, 11937-11950
20. Hille, R. (2005) Molybdenum-containing hydroxylases. *Arch Biochem Biophys* **433**, 107-116
21. Filiatrault, M. J., Picardo, K. F., Ngai, H., Passador, L., and Iglewski, B. H. (2006) Identification of *Pseudomonas aeruginosa* genes involved in virulence and anaerobic growth. *Infect Immun* **74**, 4237-4245
22. Imlay, J. A. (2006) Iron-sulphur clusters and the problem with oxygen. *Mol Microbiol* **59**, 1073-1082
23. Ollagnier de Choudens, S., and Barras, F. (2017) Genetic, Biochemical, and Biophysical Methods for Studying FeS Proteins and Their Assembly. *Methods Enzymol* **595**, 1-32
24. Ollagnier-de Choudens, S., Loiseau, L., Sanakis, Y., Barras, F., and Fontecave, M. (2005) Quinolinate synthetase, an iron-sulfur enzyme in NAD biosynthesis. *FEBS Lett* **579**, 3737-3743
25. Groenewold, M. K., Massmig, M., Hebecker, S., Danne, L., Magnowska, Z., Nimtz, M., Narberhaus, F., Jahn, D., Heinz, D. W., Jansch, L., and Moser, J. (2018) A phosphatidic acid-binding protein is important for lipid homeostasis and adaptation to anaerobic biofilm conditions in *Pseudomonas aeruginosa*. *Biochem J* **475**, 1885-1907
26. Dowhan, W. (1997) Molecular basis for membrane phospholipid diversity: why are there so many lipids? *Annu Rev Biochem* **66**, 199-232
27. Sharma, P., Teixeira de Mattos, M. J., Hellingwerf, K. J., and Bekker, M. (2012) On the function of the various quinone species in *Escherichia coli*. *FEBS J* **279**, 3364-3373
28. Nitzschke, A., and Bettenbrock, K. (2018) All three quinone species play distinct roles in ensuring optimal growth under aerobic and fermentative conditions in *E. coli* K12. *PLoS One* **13**, e0194699
29. Filiatrault, M. J., Wagner, V. E., Bushnell, D., Haidaris, C. G., Iglewski, B. H., and Passador, L. (2005) Effect of anaerobiosis and nitrate on gene expression in *Pseudomonas aeruginosa*. *Infect Immun* **73**, 3764-3772
30. Wu, M., Guina, T., Brittnacher, M., Nguyen, H., Eng, J., and Miller, S. I. (2005) The *Pseudomonas aeruginosa* proteome during anaerobic growth. *J Bacteriol* **187**, 8185-8190
31. Worlitzsch, D., Tarran, R., Ulrich, M., Schwab, U., Cekici, A., Meyer, K. C., Birrer, P., Bellon, G., Berger, J., Weiss, T., Botzenhart, K., Yankaskas, J. R., Randell, S., Boucher, R. C., and

Doring, G. (2002) Effects of reduced mucus oxygen concentration in airway *Pseudomonas* infections of cystic fibrosis patients. *J Clin Invest* **109**, 317-325
32. Kolpen, M., Hansen, C. R., Bjarnsholt, T., Moser, C., Christensen, L. D., van Gennip, M., Ciofu, O., Mandsberg, L., Kharazmi, A., Doring, G., Givskov, M., Hoiby, N., and Jensen, P. O. (2010) Polymorphonuclear leucocytes consume oxygen in sputum from chronic *Pseudomonas aeruginosa* pneumonia in cystic fibrosis. *Thorax* **65**, 57-62
33. Kolpen, M., Bjarnsholt, T., Moser, C., Hansen, C. R., Rickelt, L. F., Kuhl, M., Hempel, C., Pressler, T., Hoiby, N., and Jensen, P. O. (2014) Nitric oxide production by polymorphonuclear leucocytes in infected cystic fibrosis sputum consumes oxygen. *Clin Exp Immunol* **177**, 310-319
34. Linnane, S. J., Keatings, V. M., Costello, C. M., Moynihan, J. B., O'Connor, C. M., Fitzgerald, M. X., and McLoughlin, P. (1998) Total sputum nitrate plus nitrite is raised during acute pulmonary infection in cystic fibrosis. *Am J Respir Crit Care Med* **158**, 207-212
35. Alvarez-Ortega, C., and Harwood, C. S. (2007) Responses of *Pseudomonas aeruginosa* to low oxygen indicate that growth in the cystic fibrosis lung is by aerobic respiration. *Mol Microbiol* **65**, 153-165
36. Skurnik, D., Roux, D., Aschard, H., Cattoir, V., Yoder-Himes, D., Lory, S., and Pier, G. B. (2013) A comprehensive analysis of in vitro and in vivo genetic fitness of Pseudomonas aeruginosa using high-throughput sequencing of transposon libraries. *PLoS Pathog* **9**, e1003582
37. Navais, R., Mendez, J., Perez-Pascual, D., Cascales, D., and Guijarro, J. A. (2014) The *yrpAB* operon of *Yersinia ruckeri* encoding two putative U32 peptidases is involved in virulence and induced under microaerobic conditions. *Virulence* **5**, 619-624
38. Sakai, Y., Kimura, S., and Suzuki, T. (2019) Dual pathways of tRNA hydroxylation ensure efficient translation by expanding decoding capability. *Nat Commun* **10**, 2858
39. Lauhon, C. T. (2019) Identification and Characterization of Genes Required for 5-Hydroxyuridine Synthesis in *Bacillus subtilis* and *Escherichia coli* tRNA. *J Bacteriol* **201**
40. Aussel, L., Loiseau, L., Hajj Chehade, M., Pocachard, B., Fontecave, M., Pierrel, F., and Barras, F. (2014) ubiJ, a new gene required for aerobic growth and proliferation in macrophage, is involved in coenzyme Q biosynthesis in *Escherichia coli* and *Salmonella enterica serovar Typhimurium*. *J Bacteriol* **196**, 70-79
41. Held, K., Ramage, E., Jacobs, M., Gallagher, L., and Manoil, C. (2012) Sequence-verified two-allele transposon mutant library for *Pseudomonas aeruginosa* PAO1. *J Bacteriol* **194**, 6387-6389
42. Jacobs, M. A., Alwood, A., Thaipisuttikul, I., Spencer, D., Haugen, E., Ernst, S., Will, O., Kaul, R., Raymond, C., Levy, R., Chun-Rong, L., Guenthner, D., Bovee, D., Olson, M. V., and Manoil, C. (2003) Comprehensive transposon mutant library of *Pseudomonas aeruginosa*. *Proc Natl Acad Sci U S A* **100**, 14339-14344
43. Wagner, V. E., Bushnell, D., Passador, L., Brooks, A. I., and Iglewski, B. H. (2003) Microarray analysis of *Pseudomonas aeruginosa* quorum-sensing regulons: effects of growth phase and environment. *J Bacteriol* **185**, 2080-2095
44. Hassett, D. J. (1996) Anaerobic production of alginate by *Pseudomonas aeruginosa*: alginate restricts diffusion of oxygen. *J Bacteriol* **178**, 7322-7325
45. Jeong, J. Y., Yim, H. S., Ryu, J. Y., Lee, H. S., Lee, J. H., Seen, D. S., and Kang, S. G. (2012) One-step sequence- and ligation-independent cloning as a rapid and versatile cloning method for functional genomics studies. *Appl Environ Microbiol* **78**, 5440-5443
46. Figurski, D. H., and Helinski, D. R. (1979) Replication of an origin-containing derivative of plasmid RK2 dependent on a plasmid function provided in trans. *Proc Natl Acad Sci U S A* **76**, 1648-1652
47. Kavran, J. M., Klein, D. E., Lee, A., Falasca, M., Isakoff, S. J., Skolnik, E. Y., and Lemmon, M. A. (1998) Specificity and promiscuity in phosphoinositide binding by pleckstrin homology domains. *J Biol Chem* **273**, 30497-30508
48. Fish, W. W. (1988) Rapid colorimetric micromethod for the quantitation of complexed iron in biological samples. *Methods in enzymology* **158**, 357-364
49. Beinert, H. (1983) Semi-micro methods for analysis of labile sulfide and of labile sulfide plus sulfane sulfur in unusually stable iron-sulfur proteins. *Analytical biochemistry* **131**, 373-378

Figure 1

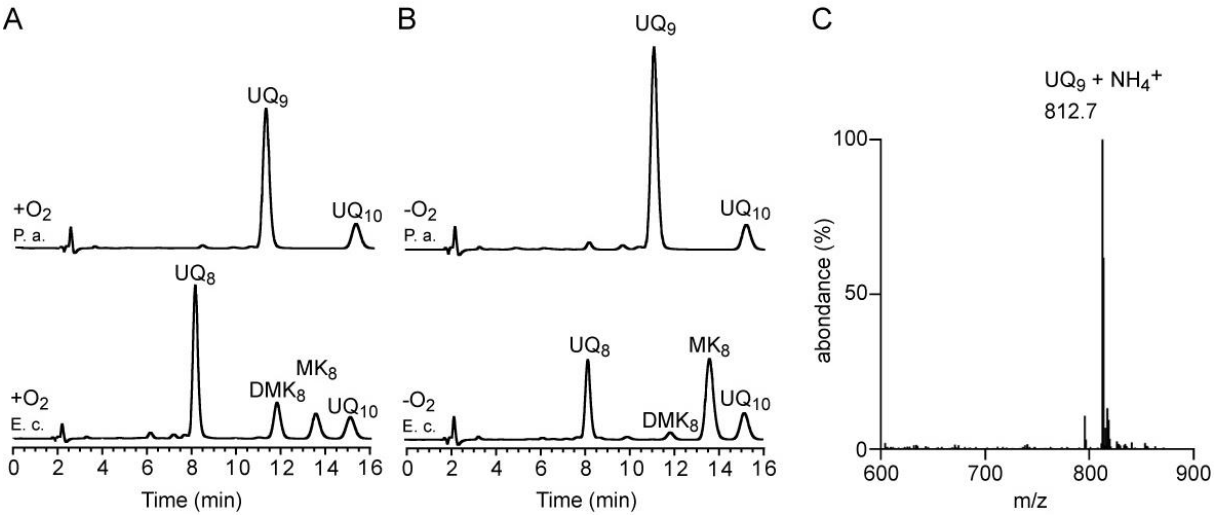
A
B
C
UQ9
+O2
P. a.
UQ10
UQ8
MK8
DMK8
+O2
E. c.
-O2
P. a.
-O2
E. c.
0 2 4 6 8 10 12 14 16
Time (min)
UQ9 + NH4+
812.7
100
50
0
abondance (%)
600 700 800 900
m/z

Figure 2

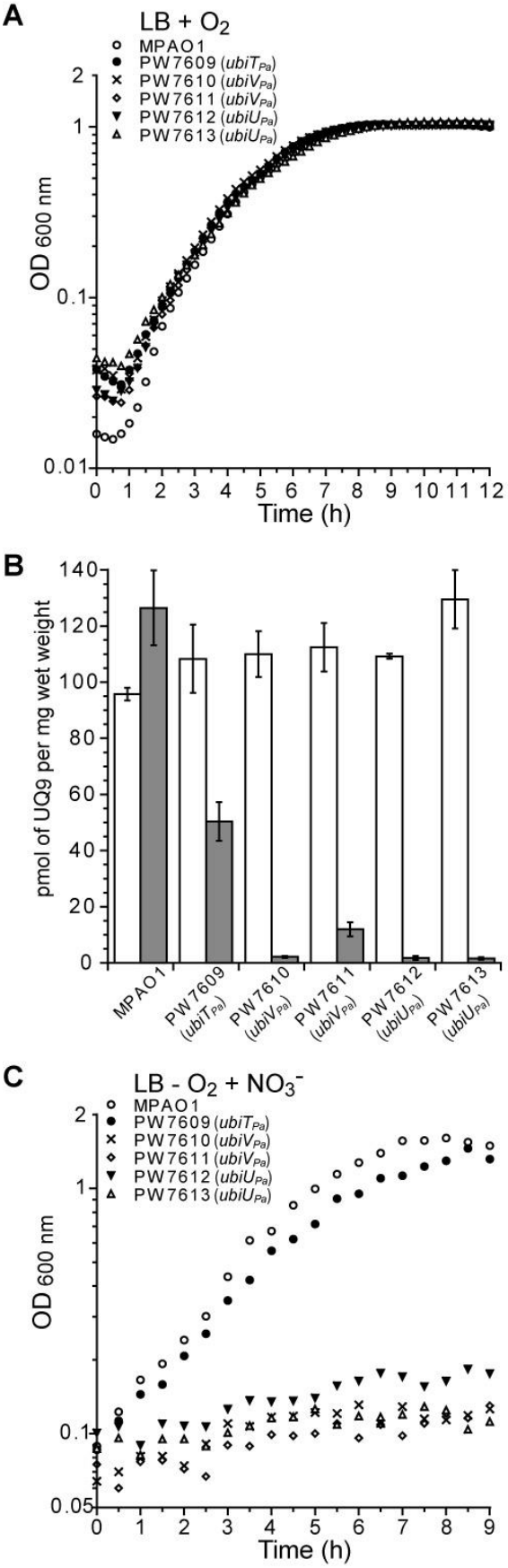

Figure 3

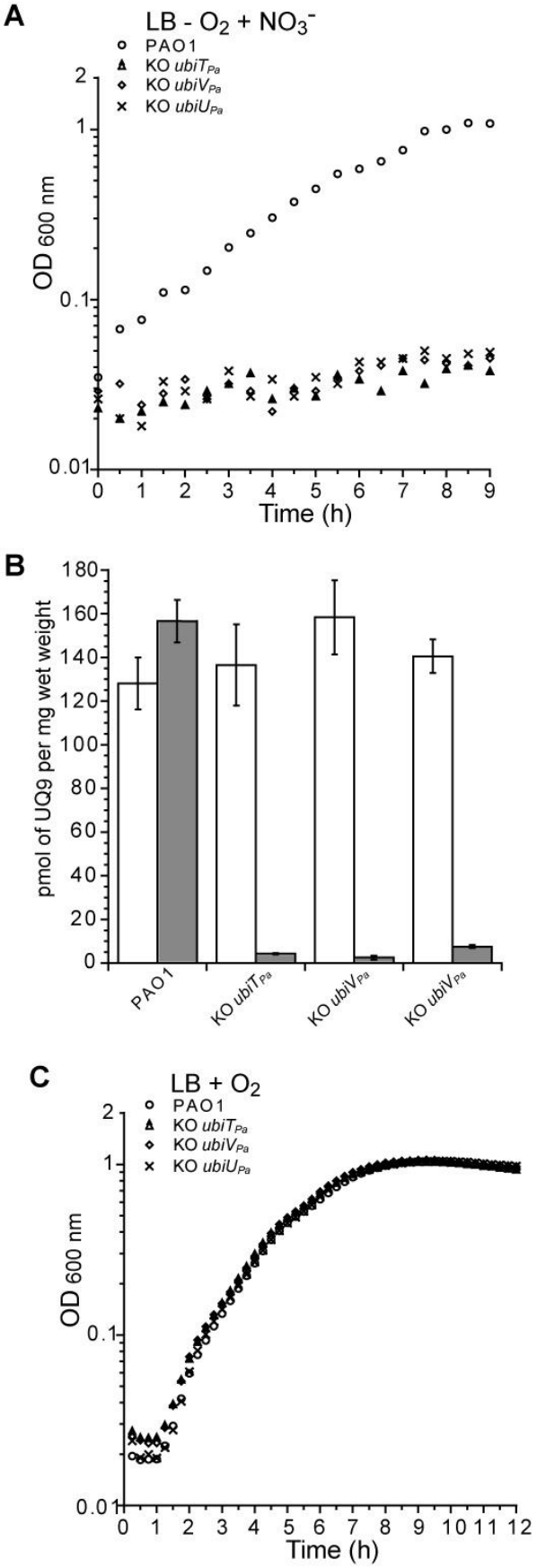

Figure 4

A

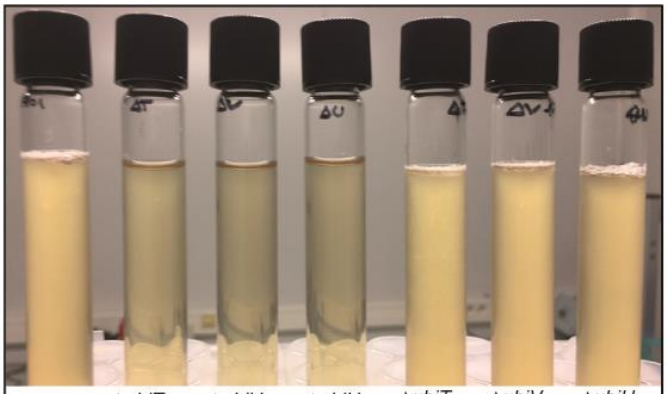

	PAO1	Δ*ubiT*$_{Pa}$ + pSW196	Δ*ubiV*$_{Pa}$ + pSW196	Δ*ubiU*$_{Pa}$ + pSW196	Δ*ubiT*$_{Pa}$ + p*ubiT*$_{Pa}$	Δ*ubiV*$_{Pa}$ + p*ubiV*$_{Pa}$	Δ*ubiU*$_{Pa}$ + p*ubiU*$_{Pa}$
UQ_9 (pmol/mg cells)	149 ±11	< 3	< 3	< 3	138 ±6	146 ±26	133 ±13

B

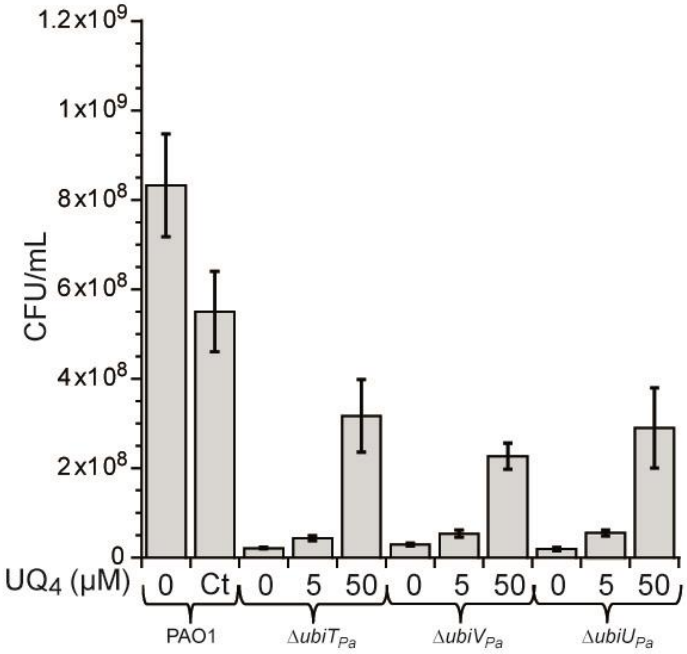

C

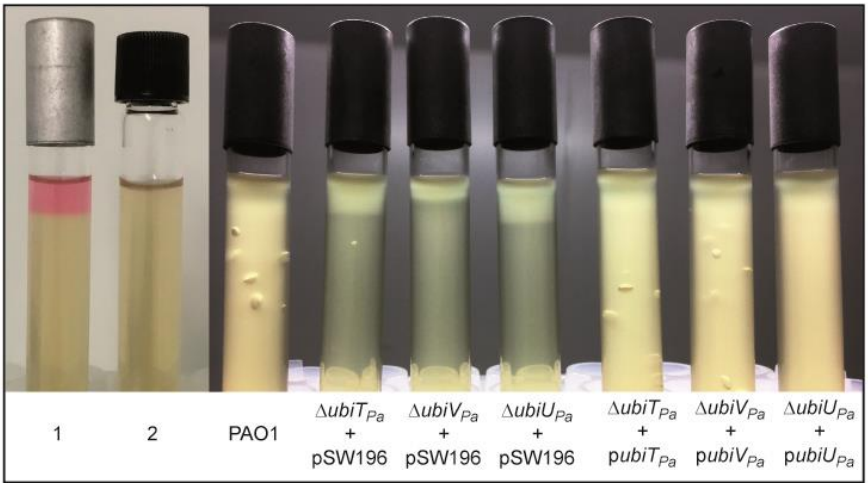

Figure 5

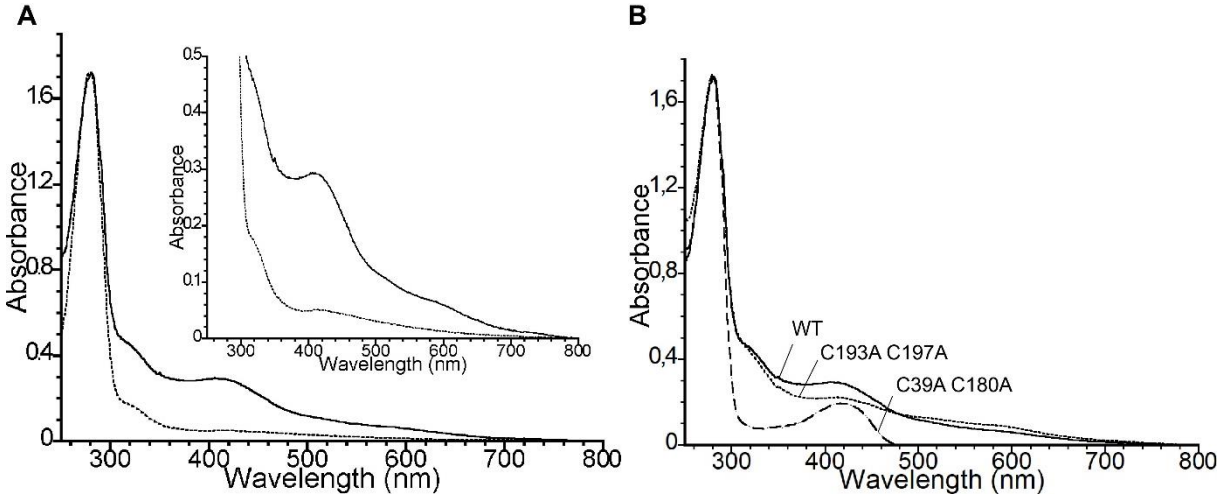

Figure 6

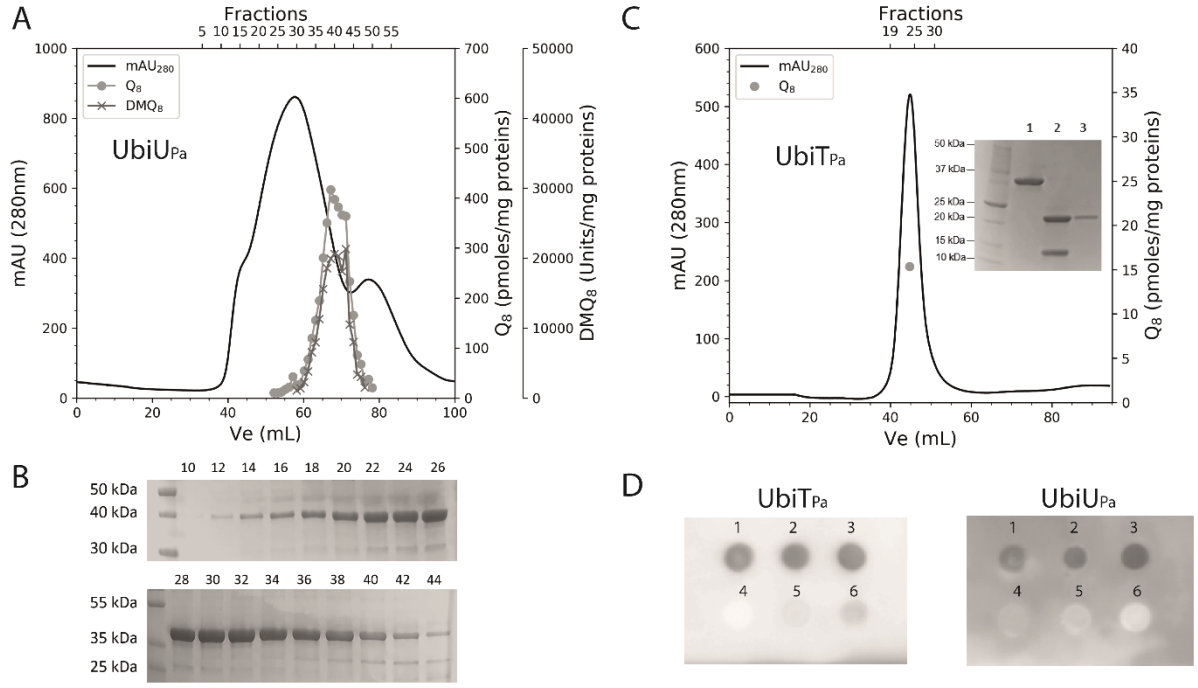

Figure S1

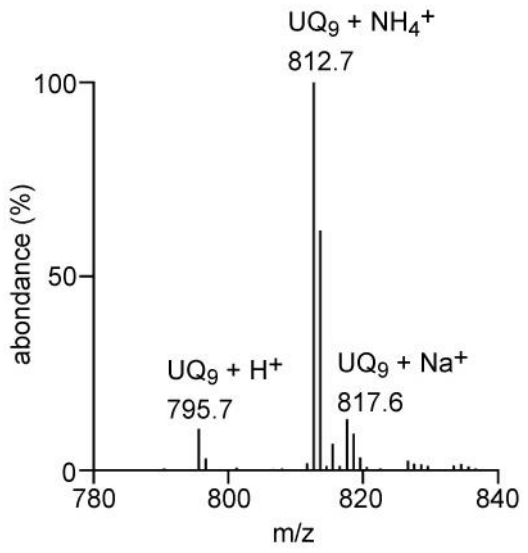

Figure S2

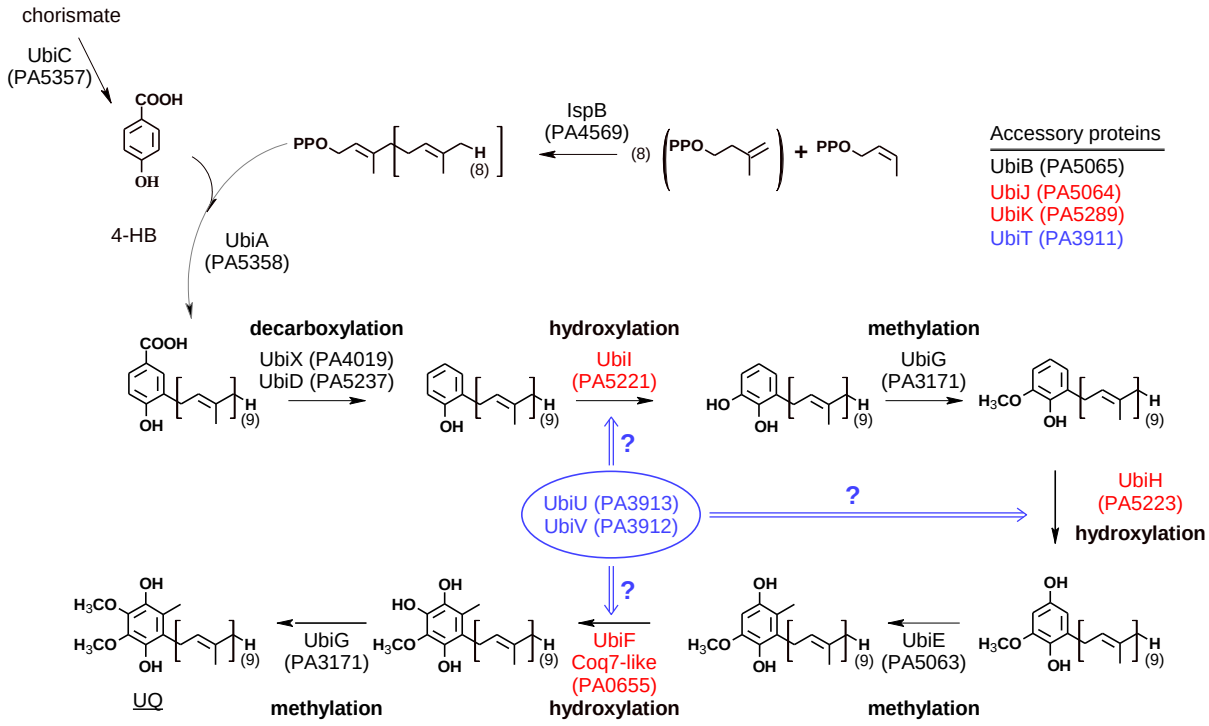

Figure S3

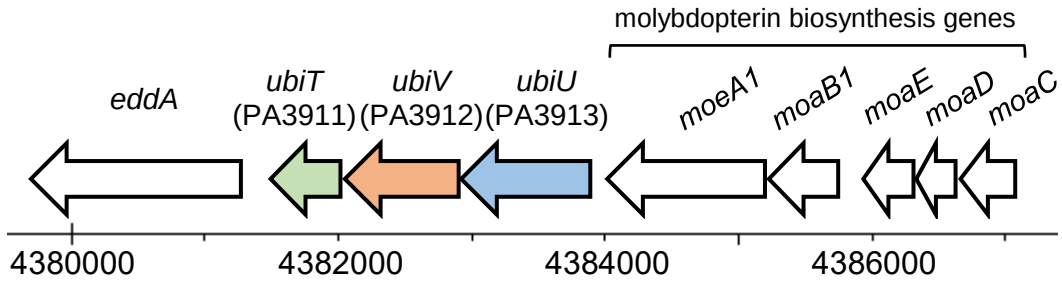

Figure S4

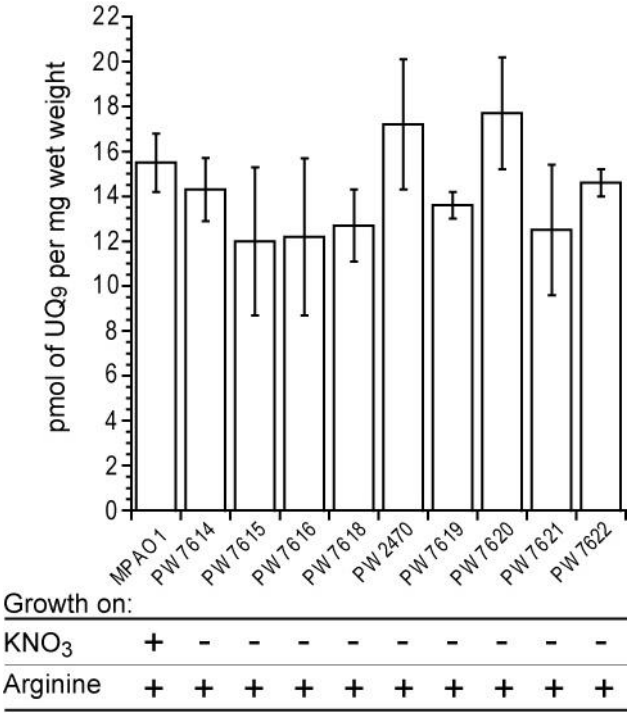

Figure S5

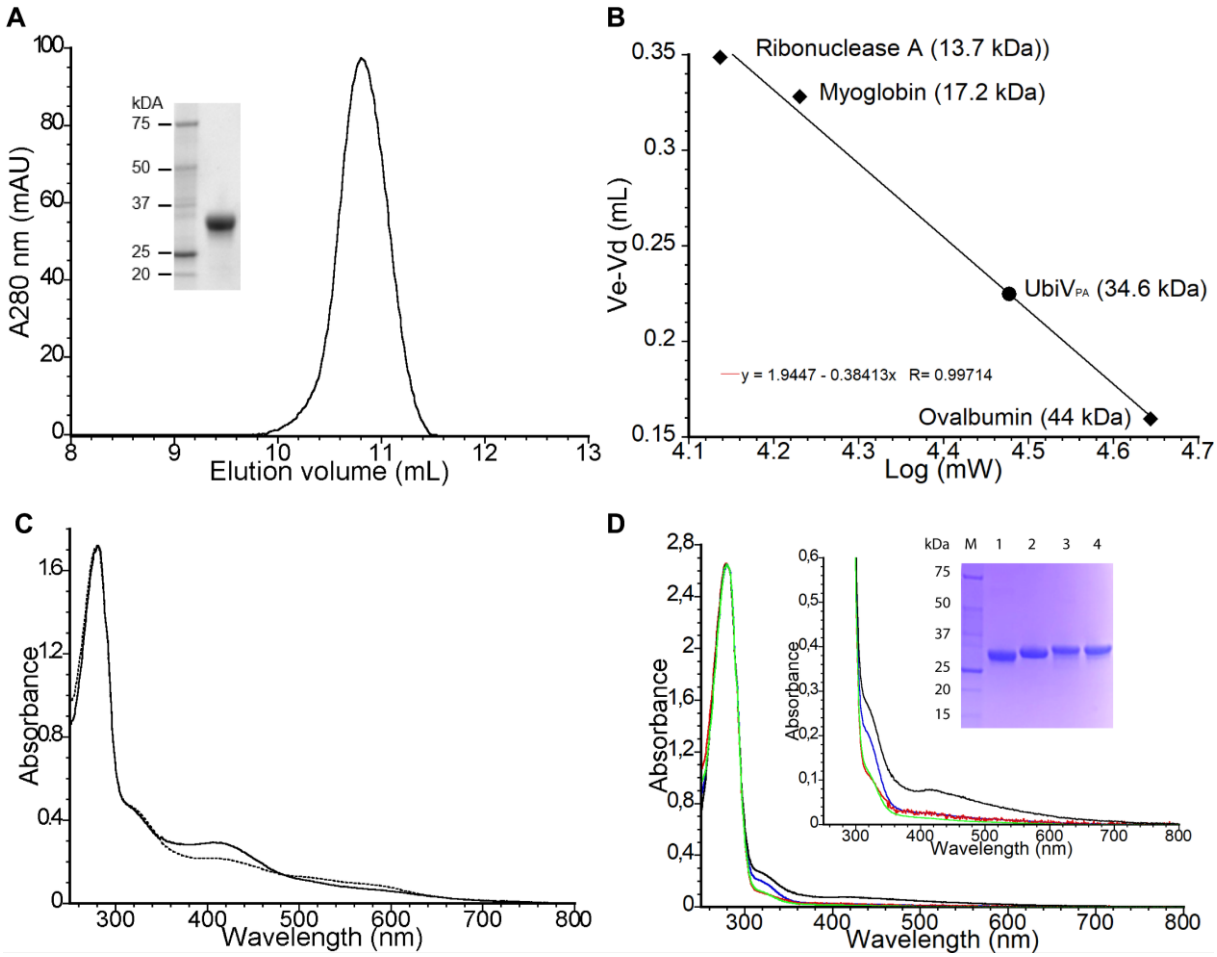

Figure S6

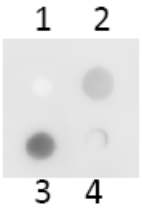

Table 1: Biochemical characterization of $UbiV_{Pa}$.

Proteins	A_{280}/A_{410}	Content (nmoles/nmole of protein)[1]	
		Iron	Sulfur
$UbiV_{Pa}$ WT	5.8	3.9 ± 0.03	3.4 ± 0.2
$UbiV_{Pa}$ C39A C180A	9.0	1.1 ± 0.16	1.6 ± 0.19
$UbiV_{Pa}$ C193A C197A	7.8	2.9 ± 0.05	3.0 ± 0.12
$UbiV_{Pa}$ C39A C193A C197A	nd	nd	nd

[1]Iron ans sulfur quantification of $UbiV_{Pa}$. Shown are metal content and UV-vis properties after naerobic reconstitution of their [Fe-S] clusters for both wild-type and mutant proteins. nd: not determinated.

Table S1: Bioinformatics analysis of the genes required for UQ synthesis in *E. coli* and *P. aeruginosa*. [1] From https://ecocyc.org/.

E. coli MG1655				*P. aeruginosa* PA01			
Gene ID	Size (aa)	Need in UQ biosynthesis (1)		Gene ID	Size (aa)	% of identity	Functions in *E. coli* [1] or specific to *P. aeruginosa*
		$+O_2$	$-O_2$				
ispB	323	Yes		*PA4569*	321	52	*all-trans*-octaprenyl-diphosphate synthase
ubiA	290	Yes		*PA5358*	296	56	4-HB octaprenyl transferase
ubiB	546	Yes		*PA5065*	533	56	Essential to UQ biosynthesis
ubiC	165	Yes		*PA5357*	178	31	Chorismate pyruvate lyase
ubiD	497	Yes		*PA5237*	496	77	3-octaprenyl 4-HB decarboxylase
ubiE	251	Yes		*PA5063*	256	73	2-octaprenyl-6-methoxy-1,4-benzoquinone methylase
ubiF	391	Yes		No homologue			2-octaprenyl-3-methyl-6-methoxy-1,4-benzoquinol hydroxylase
coq7	No homologue			*PA0655*	116	-	2-nonaprenyl-3-methyl-6-methoxy-1,4-benzoquinol hydroxylase (2)
ubiG	240	Yes		*PA3171*	232	64	3-demethylubiquinone-*8* 3-*O*-methyl transferase 2-octaprenyl-6-hydroxyphenol methylase
ubiH	392	Yes	No	*PA5223*	394	40	2-octaprenyl-6-methoxyphenol hydroxylase
ubiI	400	Yes	No	*PA5221*	405	45	2-octaprenylphenol hydroxylase
ubiJ	201	Yes	No	*PA5064*	208	21	Essential to UQ biosynthesis-SCP2 domain
ubiK	96	Yes	No	*PA5289*	86	37	Ubiquinone biosynthesis accessory factor
ubiT	174	No	Yes	*PA3911*	171	42	Essential to UQ biosynthesis-SCP2 domain
ubiU	331	No	Yes	*PA3913*	331	64	Essential to UQ
ubiV	292	No	Yes	*PA3912*	296	50	Essential to UQ
ubiX	189	Yes		*PA4019*	209	40	Flavin prenyltransferase - UbiD partner protein

1. Pelosi, L., Vo, C. D., Abby, S. S., Loiseau, L., Rascalou, B., Hajj Chehade, M., Faivre, B., Gousse, M., Chenal, C., Touati, N., Binet, L., Cornu, D., Fyfe, C. D., Fontecave, M., Barras, F., Lombard, M., and Pierrel, F. (2019) Ubiquinone Biosynthesis over the Entire O2 Range: Characterization of a Conserved O2-Independent Pathway. *mBio* **10**
2. Stenmark, P., Grunler, J., Mattsson, J., Sindelar, P. J., Nordlund, P., and Berthold, D. A. (2001) A new member of the family of di-iron carboxylate proteins. Coq7 (clk-1), a membrane-bound hydroxylase involved in ubiquinone biosynthesis. *J Biol Chem* **276**, 33297-33300

Table S2: Bacterial strains and plasmids used in this work.

Strain or plasmid			Genotype or relevant properties		Reference or source
Strains					
P. aeruginosa					
MPAO1			Wild-type strain		Manoil laboratory collection
Tn mutant	Gene ID	Name	Location	Tn position in the ORF	
PW7609	*PA3911*	-	C03::IS*phoA*/hah, Tc^R	5(516)	(1)
PW7610	*PA3912*	-	D02::IS*phoA*/hah, Tc^R	757(891)	
PW7611	*PA3912*	-	B03::IS*phoA*/hah, Tc^R	565(891)	
PW7612	*PA3913*	-	A05::IS*phoA*/hah, Tc^R	848(996)	
PW7613	*PA3913*	-	G03::IS*phoA*/hah, Tc^R	573(996)	
PW7614	*PA3914*	*moeA1*	H08::IS*phoA*/hah, Tc^R	977(1224)	
PW7615	*PA3915*	*moaB1*	F12::IS*phoA*/hah, Tc^R	403(558)	
PW7616	*PA3915*	*moaB1*	E02::IS*phoA*/hah, Tc^R	513(558)	
PW7618	*PA3916*	*moaE*	F06::IS*phoA*/hah, Tc^R	218(453)	
PW2470	*PA3916*	*moaE*	C07::IS*phoA*/hah, Tc^R	217(453)	
PW7619	*PA3917*	*moaD*	G12::IS*phoA*/hah, Tc^R	249(252)	
PW7620	*PA3917*	*moaD*	D02::IS*phoA*/hah, Tc^R	61(252)	
PW7621	*PA3918*	*moaC*	B07::IS*lacZ*/hah, Tc^R	150(483)	
PW7622	*PA3918*	*moaC*	H11::IS*phoA*/hah, Tc^R	209(483)	
PAO1			Wound isolate, sequenced laboratory strain		ref "J. Mougous"
Δ*ubiT*$_{Pa}$			PAO1 with non-polar *ubiT* (*PA3911*) deletion		This work
Δ*ubiU*$_{Pa}$			PAO1 with non-polar *ubiU* (*PA3913*) deletion		This work
Δ*ubiV*$_{Pa}$			PAO1 with non-polar *ubiV* (*PA3912*) deletion		This work
E. coli					
Top10			Chemically competent cells		Invitrogen
MG1655			Wild-type strain		Laboratory collection
BL21 (DE3) Δ*ubiUV*			as BL21 (DE3) but Δ*ubiU-ubiV*::Kan (KnR)		This work

Plasmids		
pRK2013	Helper plasmid with conjugative properties (Kn^R)	(2)
pEXG2	Allelic exchange vector (Gm^R)	(3)
pEXG2-Mut-*ubiT*$_{Pa}$	pEXG2 carrying SLIC fragment for *ubiT*$_{Pa}$ deletion	This work
pEXG2-Mut-*ubiU*$_{Pa}$	pEXG2 carrying SLIC fragment for *ubiU*$_{Pa}$ deletion	This work
pEXG2-Mut-*ubiV*$_{Pa}$	pEXG2 carrying SLIC fragment for *ubiV*$_{Pa}$ deletion	This work
pSW196	Integrative plasmid at the *attB* site, P_{BAD}-based vector for inducible gene expression (Tc^R)	(4)
p*ubiT*$_{Pa}$	pSW196 carrying P_{BAD}-*ubiT*$_{Pa}$	This work
p*ubiU*$_{Pa}$	pSW196 carrying P_{BAD}-*ubiU*$_{Pa}$	This work
p*ubiV*$_{Pa}$	pSW196 carrying P_{BAD}-*ubiV*$_{Pa}$	This work
pET22-UbiV$_{Pa}$	pET22b(+) carrying *ubiV*$_{PA}$ gene (Cter His tag)	This work
pET22-UbiV$_{Pa}$ C39A C180A	pET22b(+) carrying *ubiV*$_{PA}$ gene with double mutation C39A and C180A (Cter His tag)	This work
pET22-UbiV$_{Pa}$ C193A C197A	pET22b(+) carrying *ubiV*$_{PA}$ gene with double mutation C193A and C197A (Cter His tag)	This work
pET22-UbiV$_{Pa}$ C39A C193A C197A	pET22b(+) carrying *ubiV*$_{PA}$ gene with triple mutation C39A, C193A and C197A (Cter His tag)	This work
pET22-UbiU$_{Pa}$	pET22b(+) carrying *ubiU*$_{PA}$ gene (Cter His tag)	This work
pET22-UbiT$_{Pa}$	pET22a(+) carrying *ubiT*$_{PA}$ gene (fused with the thioredoxin DNA)	This work

1. Jacobs, M. A., Alwood, A., Thaipisuttikul, I., Spencer, D., Haugen, E., Ernst, S., Will, O., Kaul, R., Raymond, C., Levy, R., Chun-Rong, L., Guenthner, D., Bovee, D., Olson, M. V., and Manoil, C. (2003) Comprehensive transposon mutant library of *Pseudomonas aeruginosa*. *Proc Natl Acad Sci U S A* **100**, 14339-14344
2. Figurski, D. H., and Helinski, D. R. (1979) Replication of an origin-containing derivative of plasmid RK2 dependent on a plasmid function provided in trans. *Proc Natl Acad Sci U S A* **76**, 1648-1652
3. Rietsch, A., Vallet-Gely, I., Dove, S. L., and Mekalanos, J. J. (2005) ExsE, a secreted regulator of type III secretion genes in *Pseudomonas aeruginosa*. *Proc Natl Acad Sci U S A* **102**, 8006-8011
4. Baynham, P. J., Ramsey, D. M., Gvozdyev, B. V., Cordonnier, E. M., and Wozniak, D. J. (2006) The *Pseudomonas aeruginosa* ribbon-helix-helix DNA-binding protein AlgZ (AmrZ) controls twitching motility and biogenesis of type IV pili. *J Bacteriol* **188**, 132-140

Table S3: Isoprenoid quinones content of the SEC-purified Ubi_{Pa}, proteins.

Purified proteins	UQ_8 (pmol/mg proteins)	DMQ_8 (AU/mg proteins)
$UbiV_{Pa}$	nd	nd
$UbiT_{Pa}$[1]	9.75±4.57	nd
$UbiU_{Pa\ (39)}$ [2]	488.17	19932
$UbiU_{Pa\ (40)}$ [2]	457.06	20603

Quantification by HPLC-MS (monitoring of NH_4^+ adducts) of DMQ_8 and UQ_8. [1] Data obtained from three independent purifications. [2] Isoprenoid quinone content corresponding to the fractions 39 and 40 of the SEC elution profil (see Fig. 6A). nd: non detected. AU: arbitrary unit.

Table S4: Primers used in this work. Restriction sites are underlined.

Name	Sequence (5'→3')	Use
Mut-ubiT-F1	GGTCGACTCTAGAGGATCCCCTATTCCTGGGG CATGCGCCGC	*ubiT*$_{Pa}$ deletion
Mut-ubiT-R1	ACGCCCCTTTCCACCGACCTCAGCTCAGCATA GCCCTGCCTCCTCTG	*ubiT*$_{Pa}$ deletion
Mut-ubiT-F2	GCTGAGGTCGGTGGAAAGGGG	*ubiT*$_{Pa}$ deletion
Mut-ubiT-R2	ACCGAATTCGAGCTCGAGCCCCGAGACCAGCC GACGCGGCT	*ubiT*$_{Pa}$ deletion
Mut-ubiU-F1	GGTCGACTCTAGAGGATCCCCTGGCGATCCAG CCGGGCAAG	*ubiU*$_{Pa}$ deletion
Mut-ubiU-R1	CTCAGTTTCATCGCGGCGGTCCTCACATGGGGT TGCTCCTCTGGCG	*ubiU*$_{Pa}$ deletion
Mut-ubiU-F2	TGAGGACCGCCGCGATGAAACT	*ubiU*$_{Pa}$ deletion
Mut-ubiU-R2	ACCGAATTCGAGCTCGAGCCCCTGCAATTGCT CCAGGCCCAG	*ubiU*$_{Pa}$ deletion
Mut-ubiV-F1	GGTCGACTCTAGAGGATCCCCATCATGGCCGA GGGCCGCTG	*ubiV*$_{Pa}$ deletion
Mut-ubiV-R1	TCAGCATAGCCCTGCCTCCTCCATCGCGGCGGT CCTCACTGCCA	*ubiV*$_{Pa}$ deletion
Mut-ubiV-F2	GAGGAGGCAGGGCTATGCTGA	*ubiV*$_{Pa}$ deletion
Mut-ubiV-R2	ACCGAATTCGAGCTCGAGCCCCCCTGGACCGG CCCCTGGG	*ubiV*$_{Pa}$ deletion
ubiT-PA-F	GGGGAATTCGGGGATGCTGCGGGCAGAGGAG GCA	*ubiT*$_{Pa}$ complementation
ubiT-PA-R	GGGGAGCTCTCAGCCGCCCCGCGCGCCC	*ubiT*$_{Pa}$ complementation
ubiU-PA-F	GGGGAATTCGAGCGCGTTTTTCGCCAGAGGA	*ubiU*$_{Pa}$ complementation
ubiU-PA-R	GGGGAGCTCTCACTGCCAGGAACGGTGATAGG	*ubiU*$_{Pa}$ complementation
ubiV-PA-F	GGGGAATTCTCACCGTTCCTGGCAGTGAGGAC CG	*ubiV*$_{Pa}$ complementation
ubiV-PA-R	GGGGAGCTCTCAGCATAGCCCTGCCTCCTCTG CC	*ubiV*$_{Pa}$ complementation
pET22-ubiV-F	GGGGCATATGAAACTGAGCCTGGGACCGCTGC TGTTCTAC	pET22-UbiV$_{Pa}$
pET22-ubiV-R	TTTTCTCGAGGCATAGCCCTGCCTCCTCTGCCC GCA	
pET22-UbiU-F	AAAACATATGCAACTGGTCTGTCCGGCGGGCA GCCT	pET22-UbiU$_{Pa}$
pET22-UbiU-R	CCCCCTCGAGCTGCCAGGAACGGTGATAGGCG CCCAGG	
pET32-UbiT-F	TTTTGAATTCATGCTGAATCGTCAGCGTCTGCT GCTGGGT	pET32-UbiT$_{Pa}$
pET22-UbiT-R	CCCCGCGGCCGCTTAACCACCACGTGCACCCT GAACCGGAC	
UbiV-C193AC197A-F	TGCGCCCAGCAGTATCCCGAAGG	pET22-UbiV$_{Pa}$ C193A C197A
UbiV-C193AC197A-R	GAACTGAGCGTCGTCCTTGGGC	
UbiV-C39A-F	GCGCCGGGCGCTGTCCCTGAACGATTG	pET22-UbiV$_{Pa}$ C39A C180A
UbiV-C39A-R	TTGGCGGCGACGGTCTCGCCGAGGTAGATG	
UbiV-C180A-F	CTGGCCTACTCGGCGCGCGCCTTCACCGCGCG GGCGGAGAACCG	pET22-UbiV$_{Pa}$ C180A
UbiV-C180A-R	CGGTTCTCCGCCCGCGCGGTGAAGGCGCGCGC CGAGTAGGCCAG	